DOI: 10.1002/chem.200500619

# Photophysics of a Series of Efficient Fluorescent pH Probes for Dual-Emission-Wavelength Measurements in Aqueous Solutions

**Sandrine Charier,[a] Odile Ruel,[a] Jean-Bernard Baudin,[a] Damien Alcor,[a] Jean-François Allemand,[b] Adrien Meglio,[a] Ludovic Jullien,*[a] and Bernard Valeur[c]**

**Abstract:** This paper evaluates the 5-aryl-2-pyridyloxazole backbone to engineer donor–acceptor fluorescent pH probes after one- or two-photon absorption. Parent fluorophores, as well as derivatives that can be used to label biomolecules, can be easily obtained in good yields. These molecules exhibit a large one-photon absorption in the near-UV range, and a strong fluorescence emission that covers the whole visible domain. The 5-aryl-2-pyridyloxazole derivatives also possess significant cross sections for two-photon absorption. Upon pyridine protonation, large shifts were observed in the absorption spectra after one- and two-photon excitation, as well as in the emission spectra. This feature was used to measure the p$K_a$ of the investigated compounds that range between 2 and 8. In most of the investigated derivatives, the p$K_a$ increased upon light excitation and protonation exchanges took place during the lifetime of the excited state, as shown by phase-modulation fluorometry analysis. Several 5-aryl-2-pyridyloxazole derivatives are suggested as efficient probes to reliably measure the pH of aqueous solutions by means of ratiometric methods that are dependent on fluorescence emission.

**Keywords:** fluorescent probes · nitrogen heterocycles · pOH-jump molecules · sensors · structure–activity relationships

## Introduction

The various synthetic and natural fluorescent molecules available have found use in many applications: fluorophores are increasingly used as reporter molecules for labeling, for sensing, and for evaluating intramolecular distances or molecular motions, for example.[1,2] This is especially true for the field of biology in which fluorescence microscopy has become an essential tool for investigating structures and functions both at the molecular and cellular level. Relatively small molecules exhibiting large fluorescence quantum yields with additional specific features are always sought after for such applications. Despite extensive work, only a few families of molecules satisfy the preceding criteria, as revealed by the catalogue contents of the main retailers of fluorescent molecular probes. In fact, the need for appropriate fluorescent labels or probes covering the whole UV-visible wavelength range is even regarded as critical for the development of experiments that rely on the observation of single fluorescent molecules.[3] Finally, the development of new, powerful microscopy approaches[4–7] requires the identification of fluorophores meeting specific criteria such as exhibiting large cross sections for multiple photon absorptions.[8,9]

Water-soluble fluorescent probes have been developed to measure the concentration of important biological metabo-

[a] Dr. S. Charier, Dr. O. Ruel, Dr. J.-B. Baudin, Dr. D. Alcor, A. Meglio, Prof. Dr. L. Jullien
Département de Chimie (C.N.R.S. U.M.R. 8640)
École Normale Supérieure
24, rue Lhomond, 75231 Paris Cedex 05 (France)
Fax: (+33) 1-44-32-33-25
E-mail: Ludovic.Jullien@ens.fr

[b] Dr. J.-F. Allemand
Département de Physique (C.N.R.S. U.M.R. 8550)
École Normale Supérieure
24, rue Lhomond, 75231 Paris Cedex 05 (France)

[c] Prof. Dr. B. Valeur
Laboratoire de Chimie Générale (C.N.R.S. U.M.R. 8531)
Conservatoire National des Arts et Métiers
292, rue Saint-Martin, 75141 Paris Cedex 03 (France)
and
Laboratoire PPSM, École Normale Supérieure de Cachan
61, avenue du Président Wilson, 94235 Cachan Cedex (France)

Supporting information for this article is available on the WWW under http://www.chemeurj.org/ or from the author. It contains an appendix (interpretation of the solvatochromism in absorption and fluorescence emission, and the evaluation of the protonation constant of the excited state of the oxazoles); one- and two-photon absorption and emission spectra after one-photon excitation of 4-PYPO, 2-PYMPO, 2-QUIMPO, 4-PYMPO-$NHNH_2$, 4-PYMPO-NHNHAc, 4-PYHPO, 2-PYMPO-$CO_2H$, 2-PYMPO-$CO_2Me$, 2-PYMPO-$CH_2OH$, 4-BOMPO, 4-PYMPOMe$^+$ $TsO^-$, and 4-PYMPOM (Figures 1S–12S, respectively); Stern–Volmer analysis of the lifetimes extracted from the measurements performed on solutions of 4-PYMPO below pH 3 (Figure 13S); analysis of the solvatochromism in the oxazole series in relation to acid–base reactions (Figures 14S and 15S).

   

lites such as ions. For example, these probes were used to image essential processes involving $Ca^{2+}$ ions in vivo. Despite its significance, fewer studies deal with imaging proton concentrations by using fluorescence microscopy.[10] A possible explanation for this is the absence of entirely satisfactory fluorescent indicators for measuring pH in the relevant 4.5–7.4 range.[11] In fact, the backbone structure of most existing fluorescent pH indicators (fluorescein and pyranin, for instance) does not facilitate the synthesis of fluorescent derivatives with different acid–base properties. In addition, pH does not usually modify their emission spectra significantly, it only affects the intensity of their fluorescence emission; thus, measuring a pH can be difficult when the concentration of the probe is unknown or when its fluorescence quantum yield is affected, as is frequently encountered in biology. To circumvent the latter drawbacks, dual-excitation-wavelength ratiometric measurements can be used when the absorption spectra of the fluorescent pH probe in basic and acidic states differ enough. In practice, such measurements are demanding because they require excitation at two different wavelengths. More favorable series that exhibit shifted emission from the acidic and basic states have been reported;[12] dual-emission-wavelength measurements can be performed, but the nature and the concentration of buffering species seem to alter pH determination from the emission spectra.[12] To measure pH by using fluorescence remains a delicate process and requires preliminary calibrations.

We recently introduced an efficient fluorescent indicator to measure pH in aqueous solution around neutrality by means of a ratiometric method relying on fluorescence emission after one- and two-photon excitation.[13] The present paper reports on the procedure that was followed to engineer the corresponding probe from the attractive 5-aryl-2-pyridyloxazole platform. The manuscript is organized as follows: We first discuss the design of fluorescent pH indicators based on the 2-aryl-5-aryloxazole backbone and describe their syntheses. We then present their photophysical features: most compounds exhibit satisfactory features with respect to one- and two-photon absorption, as well as to emission. The acid–base behavior of their ground state is investigated by UV-visible absorption spectra: the distribution of $pK_a$ values makes this series attractive to optically measure pH over a wide range. We subsequently examine the evolution of their emission spectra as a function of pH and perform complementary time-resolved fluorescence measurements. Despite favorable photophysical and acidobasic properties, we show that only a few 5-aryl-2-aryloxazole derivatives meet all of the constraining criteria for measuring pH by means of a ratiometric analysis of their emission spectra.

**Abstract in French:** *Cet article évalue le squelette 5-aryl-2-pyridyloxazole pour la conception de sondes fluorescentes de pH de type donneur–accepteur après excitation à un ou deux photons. Il est facile d'obtenir avec de bons rendements et en grande quantité les têtes de série tout autant que des dérivés conçus pour effectuer la fonctionnalisation de biomolécules. Ces sondes absorbent intensément la lumière dans le proche UV et présentent une forte émission de fluorescence qui couvre toute l'étendue du domaine visible. Elles possèdent aussi d'appréciables sections efficaces d'absorption à deux photons. La protonation du cycle pyridine s'accompagne de déplacements importants à la fois dans les spectres d'absorption après excitation à un et deux photons, et dans les spectres d'émission. Ces altérations sont utilisées pour mesurer le p$K_a$ des sondes synthétisées qui s'étage entre 2 et 8. Une étude par fluorimétrie de phase démontre que le p$K_a$ de la plupart de ces sondes augmente après absorption lumineuse et que des réactions acido–basiques se produisent au cours de la durée de vie de l'état excité. Ce manuscrit démontre que plusieurs 5-aryl-2-pyridyloxazoles constituent des sondes de pH efficaces et fiables pour mesurer le pH en solution aqueuse par analyse ratiométrique en émission.*

## Design and synthesis of the probes

*Design*: To measure pH by means of a ratiometric method based on fluorescence emission it is desirable (but not sufficient; see below) that the acidic and basic states of the indicator are both fluorescent and exhibit shifted absorption and emission spectra. In principle, this goal can be achieved when either the donor or the acceptor moiety of a donor–acceptor fluorophore exhibits acidic or basic properties. However, this general strategy is difficult to implement. In practice, numerous pathways compete with fluorescence emission for the relaxation of the excited state in donor–acceptor chromophores: for example, the basic donor amino groups can act as fluorescence quenchers.[1,2] An important constraint is thus to have similar fluorescence quantum yields for the acidic and the basic states of the pH indicator. In addition, the $pK_a$ values of the ground and excited states are prone to be significantly different in many donor–acceptor molecules owing to the redistribution of the electron cloud around the molecule upon light absorption.[14,15,16] This feature has been fruitfully used to generate transient out-of-equilibrium states to investigate the buffering properties of media surrounding pH- or pOH-jump probes.[17] In the present context, it considerably complicates the analysis of the pH from the ratio of emissions from the acidic and basic states of the fluorescent pH indicator (see below).

These considerations encouraged us to choose the 5-aryl-2-pyridyloxazole backbone to engineer donor–acceptor fluorescent pH probes (see Figure 1). This series, originally investigated to develop laser dyes,[18] is easy to synthesize and is prone to structural variations. It exhibits favorable photophysical features after one-photon excitation: $\varepsilon \approx 3 \times 10^4\,\text{M}^{-1}\text{cm}^{-1}$ at $\lambda \approx 350$ nm and strong fluorescence emission (quantum yield of fluorescence, $\phi$, up to 1) at $\lambda \approx 500$ nm from both pyridinium and pyridine states.[18] In fact, this backbone has already been used to design 5-(4′-methoxyphenyl)-2-(4-pyridyl)oxazole (4-PYMPO; Figure 1) as a fluorescent pH probe.[10,19,20] With respect to biological applications, the strong fluorescence as well as the shifted absorp-

  

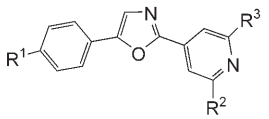

| | $R^1$ | $R^2$ | $R^3$ |
|---|---|---|---|
| 4-PYPO | H | H | H |
| 4-PYMPO | MeO | H | H |
| 4-PYHPO | HO | H | H |
| 4-PYMPO-Cl | MeO | H | Cl |
| 4-PYMPO-$NHNH_2$ | MeO | H | $NHNH_2$ |
| 4-PYMPO-$NH_2$ | MeO | H | $NH_2$ |
| 4-PYMPO-NHNHAc | MeO | H | NHNHAc |
| 4-PYMPOM | MeO | Me | Me |

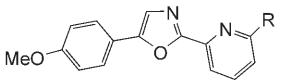

| | R |
|---|---|
| 2-PYMPO | H |
| 2-PYMPO-$CO_2H$ | $CO_2H$ |
| 2-PYMPO-$CO_2Me$ | $CO_2Me$ |
| 2-PYMPO-$CH_2OH$ | $CH_2OH$ |

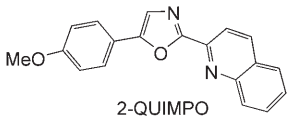

2-QUIMPO

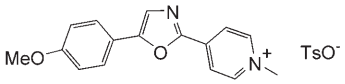

4-PYMPOMe$^+$ TsO$^-$

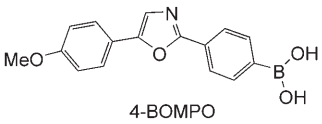

4-BOMPO

Figure 1. Generic structures of the derivatives prepared during the present study.

tion and emission spectra of the acidic and basic states of 4-PYMPO are especially attractive. However, the biological relevance of 4-PYMPO is restricted to measurements in the most acidic cellular compartments as it has a low p$K_a$ value (p$K_a \approx 4$). From the latter point of view, a related boronic acid probe with p$K_a \approx 8$[21] could increase the relevance of the 5-aryl-2-aryloxazole backbone for designing fluorescent pH probes.

We designed a series of 5-aryl-2-pyridyloxazoles aiming at the following: 1) keeping the attractive photophysical and water-solubility properties of 4-PYMPO. As far as absorption properties were concerned, we sought molecules exhibiting absorption maxima after one-photon excitation in the $\lambda = 350$–$400$ nm range. For such donor–acceptor compounds, one can expect the corresponding absorption maxima after two-photon excitation to lie between $\lambda = 700$ and 900 nm (this range is easily accessible with the commonly used sources for two-photon excitation)[22]; 2) covering the largest p$K_a$ range. We introduced different substituents on the pyridine ring by using reported p$K_a$ values as a guideline.[23] Finally, we considered the commercial availability of the synthetic precursors to accelerate the screening process devoted to extract the general trends in the present series. The latter should be helpful in refining the design of 5-aryl-2-pyridyloxazole-based fluorescent pH indicators that meet all of the constraining criteria.

Two different backbones were chosen according to the nitrogen position (2- or 4-) in the pyridine ring in the 5-aryl-2-pyridyloxazole (Figure 1). Within each series, the fluorophores differ by the length of the conjugation path and/or by the presence of donor or acceptor groups on the oxazole. In the parent 4-pyridyl fluorophores, we chose 5-phenyl-2-(4-pyridyl)oxazole (4-PYPO),[24] 4-PYMPO,[18] 5-(4′-methoxyphenyl)-2-(2,6-dimethyl-4-pyridyl)oxazole (4-PYMPOM), and 4-[5-(4′-methoxyphenyl)-2-oxazolyl]-2-pyridylamine (4-PYMPO-$NH_2$; named PYMPON in our previous communication).[13] 5-(4′-Methoxyphenyl)-2-(2-pyridyl)oxazole (2-PYMPO), 5-(4′-methoxyphenyl)-2-(2-quinolyl)oxazole (2-QUIMPO), and the methyl ester of 6-[5-(4′-methoxyphenyl)-2-oxazolyl]picolinic acid (2-PYMPO-$CO_2$Me) form the parent 2-pyridyl fluorophores.

We also considered several related derivatives: 4-PYMPO-$NHNH_2$, 4-PYHPO, 2-PYMPO-$CH_2OH$, and 2-PYMPO-$CO_2H$ (Figure 1). These compounds bear functional groups that are expected to alter the p$K_a$ of the pyridine ring either by ion–ion interaction in the pyridinium state (4-PYMPO-$NHNH_2$, 4-PYHPO, and 2-PYMPO-$CO_2H$) or through a hydrogen bond (2-PYMPO-$CH_2OH$) in the pyridine form.[25,26] In view of their functionality, such derivatives could be used to label biomolecules. In the latter case, they could also act as electrochromic fluorescent probes. In fact, the protonation extent of any acid depends on the pH, its p$K_a$, and the local electric field.[27–29] In addition, proton-exchange reactions are generally diffusion-limited.[25,26] Thus, fluorescent pH probes could provide a reasonable alternative to fast fluorescent electrochromic probes that rely on the alteration of their transition dipole moments.[30,31]

We wanted to overcome the p$K_a$ limitations intrinsic to the approach relying on substituting the pyridine ring. Despite the possible interference with solutes other than protons,[32] we were interested in the recently reported 5-(4′-dimethylaminophenyl)-2-[4-(dihydroxyboranyl)]oxazole with p$K_a \approx 8$.[21] This pH probe is strongly fluorescent in the basic state but only poorly in the corresponding acidic one. Therefore, we completed the present pyridine series with 5-(4′-methoxyphenyl)-2-[4-(dihydroxyboranyl)]oxazole (4-BOMPO; Figure 1), aiming to improve the fluorescence quantum yield of the acidic state by reducing the donating power of the donor substituent.

*Synthesis*: The condensation reaction between 4-methoxyphenacylamine and the appropriate carboxylic acid in phos-

  

phoryl chloride at reflux is the key step for building most of the 5-aryl-2-pyridyloxazole backbones in the present series of derivatives (Scheme 1).[18]

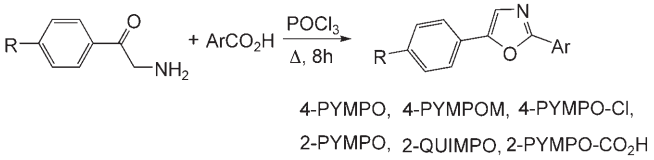


Scheme 1. General scheme of the condensation reaction leading to the formation of the 5-aryl-2-pyridyloxazole backbone.

4-PYMPO, 4-PYMPOM, 4-PYMPO-Cl, 2-PYMPO, 2-QUIMPO, and 2-PYMPO-$CO_2H$ were obtained in 87%, 60%, 88%, 63%, 39%, and 25% yields, respectively. In the case of 4-PYPO, building of the oxazole ring proceeded in two steps:[24] the condensation between phenacylamine and isonicotinic acyl chloride gave *N*-phenacylisonicotinamide (47% yield) which was reacted under reflux in a mixture of acetic anhydride and concentrated phosphoric acid to provide 4-PYPO in 33% yield. For the synthesis of 4-PYMPOM, the 2,6-dimethylisonicotinic acid precursor **4** was produced in three steps from 2,6-lutidine-1-oxyde (**1**; Scheme 2): 1) methylation with dimethyl sulfate to yield 1-methoxy-2,6-dimethylpyridinium methyl sulfate (**2**; 86%),[33] 2) nucleophilic substitution with potassium cyanide on **2** giving 4-cyano-2,6-dimethylpyridine (**3**; 43%),[33] and 3) hydrolysis of **3** to give **4** (40%).

The 5-aryl-2-pyridyloxazole backbone was subsequently altered to provide different derivatives (Scheme 3). 4-PYMPO-Cl was converted into the substituted hydrazine 4-PYMPO-$NHNH_2$ in a 41% yield by reacting it under reflux conditions with hydrazine.[34] 4-PYMPO-$NHNH_2$ was acylated with acetic anhydride to give 4-PYMPO-NHNHAc in 82% yield.[35] Conversely, 4-PYMPO-$NHNH_2$ was transformed into the aniline 4-PYMPO-$NH_2$ in 51% yield by reduction with Raney nickel in ethanol.[34] 4-PYMPO was demethylated with hydrogen bromide to give 4-PYHPO in a 56% yield.[36] 2-PYMPO-$CO_2H$ was esterified in acidic methanol leading first to 2-PYMPO-$CO_2Me$ (86% yield), which was then reduced to 2-PYMPO-$CHO_2H$ (80% yield).[37] Finally, we methylated the nitrogen atom of the pyridine ring in 4-PYMPO by reaction with methyl tosylate in toluene to get 4-PYMPOMe$^+$ TsO$^-$ (1-methyl-4-[5-(4′-methoxyphenyl)-2-oxazolyl]pyridinium *p*-toluenesulfonate; Figure 1) in a 65% yield[38] as a reference compound for the photophysical investigations.

The two-step synthesis of 4-BOMPO first involves the condensation of 4-methoxyphenacylamine with 4-(4,4,5,5-tetramethyl-1,3,2-dioxaborolan-2-yl)benzoyl chloride (31% yield).[21] This is followed by the dehydration of the resulting amide in phosphoryl chloride under reflux conditions, as already reported for the dimethylamino derivative, to give the product in a 66% yield (Scheme 4).[21]

It is worth noting that these syntheses can be performed on a large scale because they essentially involve recrystallization in the purification steps.

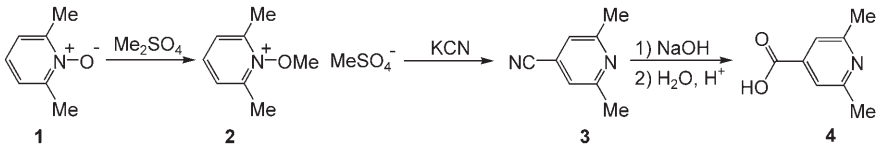


Scheme 2. Synthesis of the 2,6-dimethylisonicotinic acid precursor (**4**) used to make 4-PYMPOM.

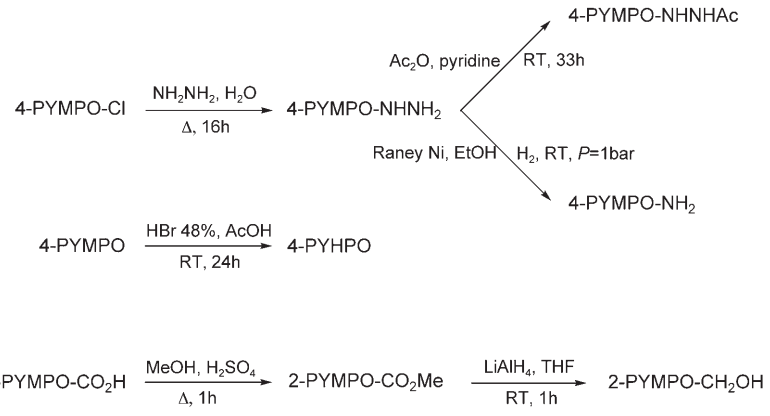


Scheme 3. Functional alterations of the 5-aryl-2-pyridyloxazole backbone.

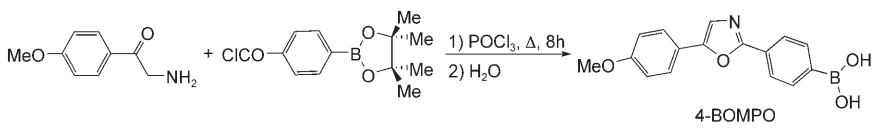


Scheme 4. Synthesis of 4-BOMPO.

## Results

**One-photon absorption**: The oxazoles presented here exhibit large one-photon absorptions ($\varepsilon \approx 2\text{–}3 \times 10^4\,M^{-1}cm^{-1}$) in a range that depends on the protonation state of the pyridine ring: ranges of $\lambda = 320\text{–}360$ and 350–430 nm were observed for the basic and acidic states, respectively (Figures 2a and 3a, Table 1, and the Supporting Information).

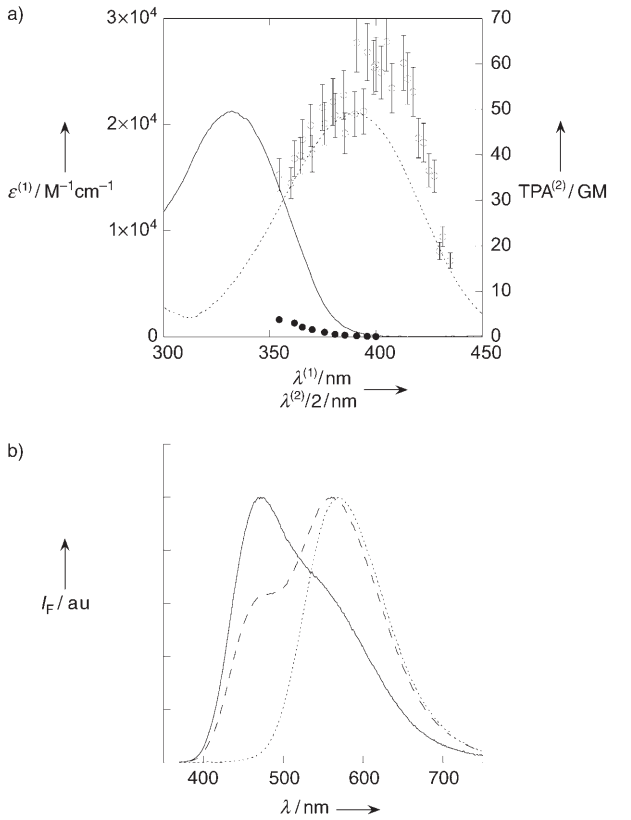


Figure 2. Photophysical properties of 4-PYMPO at 293 K. a) One-photon absorption (molar absorption coefficient, $\varepsilon$, versus $\lambda$; pH 2 = -----, pH 14 = ——) and two-photon absorptivity (TPA versus $\lambda/2$; pH 2 = ○, pH 14 = ●) spectra. b) Normalized steady-state fluorescence emission ($I_F$) after one-photon excitation at $\lambda_{exc} = 356$ nm (pH 2 = -----, pH 6 = – – –, pH 14 = ——). Solvent: Britton–Robinson buffer[53] (0.1 M).

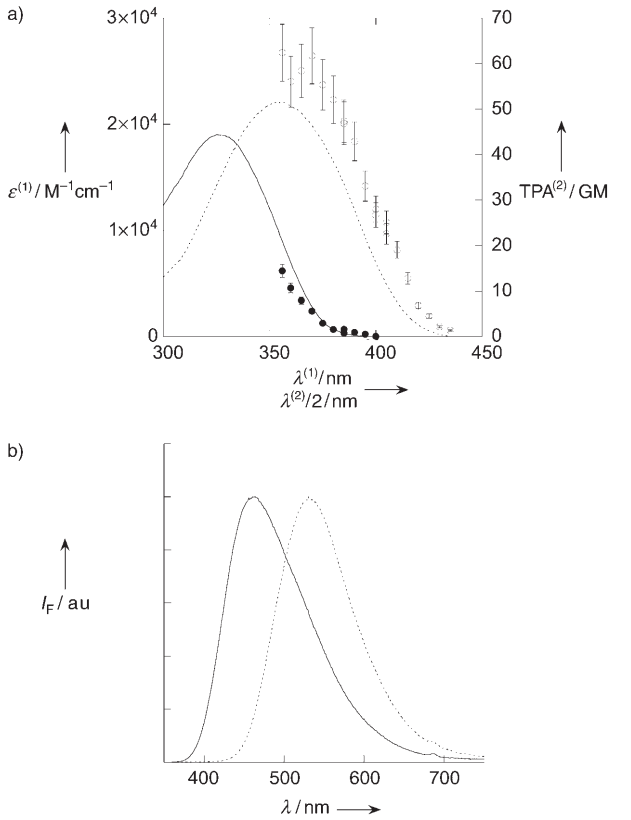


Figure 3. Photophysical properties of 4-PYMPO-$NH_2$ at 293 K. a) One-photon absorption (molar absorption coefficient, $\varepsilon$, versus $\lambda$; pH 3 = -----, pH 8 = ——) and two-photon absorptivity (TPA versus $\lambda/2$; pH 3 = ○, pH 8 = ●) spectra. b) Normalized steady-state fluorescence emission ($I_F$) after one-photon excitation at $\lambda_{exc} = 339$ nm (pH 3 = -----, pH 8 = ——). Solvent: Britton–Robinson buffer[53] (0.1 M). Adapted from ref. [13].

As anticipated, the maximum of one-photon absorption ($\lambda_{max}^{(1)}$) is redshifted when the length of the conjugation path is increased (e.g., 2-QUIMPO versus 2-PYMPO). The bathochromic shift observed by decreasing the pH is in line with the increase of the withdrawing power of the pyridine ring upon protonation of the nitrogen atom.[39] In addition, the protonated state of 4-PYMPO, that is, 4-PYMPOH$^+$, exhibits similar photophysical features to the methylammonium derivative 4-PYMPOMe$^+$ TsO$^-$. The relative position of the nitrogen atom in the pyridine ring does not significantly alter the absorption properties (e.g., 4-PYMPO versus 2-PYMPO). Substituent effects are more pronounced in the acidic state than in the basic state. For instance, 2-PYMPO, 2-PYMPO-$CO_2H$, 2-PYMPO-$CO_2Me$, and 2-PYMPO-$CH_2OH$ exhibit similar absorption features in the basic state. In contrast, the presence of an electron-donating group on a conjugated position of the aryl substituent of the oxazole ring (4-PYMPO and 4-PYHPO versus 4-PYPO) induces a pronounced redshift in the absorption of the acidic form. The absorption of the protonated state of the members of the 4-PYMPO series bearing an electron-donating nitrogen atom on the 2-position of the pyridine ring (4-PYMPO-$NHNH_2$, 4-PYMPO-NHNHAc, and 4-PYMPO-$NH_2$) is blueshifted compared with that of the parent compound 4-PYMPO. This observation is in agreement with the reduction of the withdrawing power of the pyridinium ring in the presence of a conjugated donor atom such as nitrogen. In addition, a small electrochromic effect was observed in the basic state of 4-PYMPO-$NHNH_3^+$: it absorbs at a higher wavelength than the corresponding state of 4-PYMPO-$NH_2$ owing to the close proximity of the terminal ammonium moiety.

The absorption of 4-BOMPO is less intense and significantly blueshifted relative to that of the 5-(4′-methoxyphenyl)-2-pyridyloxazoles (Table 1). The state absorbing at the largest wavelength is still the acidic state, which involves the conjugated electron-withdrawing boronic group -$B(OH)_2$. Its absorption maximum is located at a much lower wavelength than that of protonated 4-PYMPO (compare $\lambda = 323$ with 390 nm). This observation underlines the lower acceptor character of the phenylboronic group relative to the pyridinium group. In contrast, the basic state containing the boronate -$B(OH)_3^-$ group absorbs at a wavelength similar to that of the basic state of 4-PYMPO ($\lambda = 314$ instead of 332 nm).

We also recorded the UV-visible absorption spectra of 4-PYMPO, 4-PYMPO-$NH_2$, 2-PYMPO, and 4-PYMPOMe$^+$

  

Table 1. Photophysical properties of the present oxazole derivatives ($BH^+$,B). Maxima of one-photon absorption $\lambda^{(1)}_{max}$ [nm] and of steady-state fluorescence emission $\lambda^{(1)}_{em}$ [nm], molar absorption coefficients for one-photon absorption at $\lambda^{(1)}_{max}$, that is, $\varepsilon^{(1)}_{max} \pm 5\%$ [$mM^{-1}cm^{-1}$], fluorescence quantum yields $\phi_F(pH) \pm 5\%$, maxima of two-photon excitation spectra $\lambda^{(2)}_{max}$ [nm] in the investigated wavelength range ($\lambda^{(2)} = 700$–$900$ nm), and two-photon excitation cross sections at $\lambda^{(2)}_{max}$, that is, $\delta^{(2)}_{max} \pm 20\%$ [GM], in Britton–Robinson buffer[53] (0.1 M) at a given pH at 293 K.

| B | $\lambda^{(1),BH^+}_{max}(\varepsilon^{(1)}_{max})$ | $\lambda^{(1),B}_{max}(\varepsilon^{(1)}_{max})$ | $\lambda^{(1),BH^+}_{em}[\phi_F(pH)]$ | $\lambda^{(1),B}_{em}[\phi_F(pH)]$ | $\lambda^{(2),BH^+}_{max}(\delta^{(2)}_{max})$ | $\lambda^{(2),B}_{max}(\delta^{(2)}_{max})$ |
|---|---|---|---|---|---|---|
| 4-PYPO | 366(24) | 318(19) | 476[0.9(2)] | 406[0.9(12)] | 710(70) | 710(6) |
| 4-PYMPO | 390(21) | 332(21) | 569[0.3(3)] | 472[0.5(14)] | 800(65) | 710(5) |
| 4-PYMPOM | 380(19) | 330(17) | 550[0.5(3)] | 465[0.8(>14)][a] | 800(60) | 710(10) |
| 2-PYMPO | 381(24) | 328(33) | 562[0.1(1)] | 450[0.7(10)] | 780(40) | 710(20) |
| 2-QUIMPO | 427(26) | 360(21) | 616[0.05(1)] | 506[0.6(10)] | 830(40) | 740(50) |
| 4-PYMPO-$NHNH_2$[b] | 354(21) | 337(17) | 522[0.1(2)] | 501[0.6(9)] | 720(80) | 710(6) |
| 4-PYMPO-NHNHAc[c] | 368(21) | 329(13) | 544[0.4(2)] | 464[0.2(7)] | – | – |
| 4-PYMPO-$NH_2$ | 355(23) | 326(19) | 530[0.7(3)] | 465[0.8(8)] | 710(60) | 710(15) |
| 4-PYHPO[d] | 392(21) | 333(21) | 575[<0.01(2)] | 485[0.03(6)] | – | – |
| 2-PYMPO$CO_2$H[e] | – | 332(21) | – | 450[<0.01(2)] | – | – |
| 2-PYMPO$CO_2$Me | – | 333(–)[f] | 523[<0.01(1)] | 455[0.01(8)] | – | – |
| 2-PYMPO$CH_2$OH | 382(19) | 330(22) | 572[0.05(1)] | 450[0.7(9)] | 780(35) | 710(20) |
| 4-PYMPOMe$^+$ $TsO^-$[g] | 396(22) | – | 572[0.4(7)] | – | 810(65) | – |
| 4-BOMPO | 323(15) | 314(18) | 442[0.65(5)] | 398[0.65(10)] | – | – |

[a] The fluorescence emission is dominated by the emission from its protonated state even in very basic media. We added concentrated NaOH to observe the emission from the basic excited state only. [b] This is a dibase. The values given refer to the couple 4-PYMPOH$^+$-$NHNH_3^+$/4-PYMPO-$NHNH_3^+$ involving the nitrogen atom of the pyridine ring. At pH > 12, further deprotonation of the terminal ammonium -$NH_3^+$ promotes a hypsochromic shift in the absorption and emission spectra: $\lambda^{B}_{max}(\varepsilon_{max}) = 327(17)$ and $\lambda^{B}_{em}[\phi_F(pH)] = 494[0.5(12)]$. The values of the maxima of two-photon excitation are given at pH 2 and 12. [c] This is not very soluble in basic aqueous solutions. $\varepsilon_{max}$ should be taken with care. [d] 4-PYHPOH$^+$ is a diacid. The values given refer to the couple 4-PYHPOH$^+$/4-PYHPO involving the nitrogen atom of the pyridine ring. At pH > 6, further deprotonation of the hydroxyl group promotes bathochromic shifts in absorption ($\lambda^{B}_{max}(\varepsilon_{max}) = 367(20)$) and in fluorescence emission ($\lambda^{B}_{em}[\phi_F(pH)] = 640[<0.01(12)]$). [e] 2-PYMPOH$^+$-$CO_2H$ is a diacid. The values given refer to the couple 2-PYMPOH$^+$-$CO_2^-$/2-PYMPO$CO_2^-$ involving the nitrogen atom of the pyridine ring. In the absorption spectrum, any evolution associated with the deprotonation of the pyridinium moiety in the covered range of pH is not observed: the p$K_a$ of the corresponding ground state is too low. We only observed deprotonation of the carboxylic group by increasing the pH. At pH 1 where 2-PYMPO-$CO_2H$ is present: $\lambda^{BH^+}_{max}(\varepsilon_{max}) = 332(21)$, whereas $\lambda^{B}_{max}(\varepsilon_{max}) = 329(23)$ at pH 12 where 2-PYMPO-$CO_2^-$ is observed. In fluorescence emission, one first observes a poorly fluorescent state below the p$K_a$ of the carboxylic group. Emission at pH 6 ($\lambda_{em}[\phi_F] = 450[0.04]$) is tentatively attributed to the excited state 2-PYMPO-$CO_2H$*, whereas emission above pH 10 ($\lambda_{em}[\phi_F(pH)] = 450[0.05]$) is tentatively attributed to the excited state 2-PYMPO-$CO_2^-$*; see text. [f] This is not very soluble in basic aqueous solution. We chose not to give any value of $\varepsilon_{max}$. [g] The experiments were performed in buffer at pH 7.

$TsO^-$ in several solvents (Table 2). The latter shares photophysical features closely related to those of 4-PYMPOH$^+$. In addition, it is more soluble in organic solvents. The one-photon absorption maximum is not sensitive to solvent polarity for the basic states (4-PYMPO, 4-PYMPO-$NH_2$, and 2-PYMPO), whereas it slightly drops when the solvent polarity is increased for 4-PYMPOMe$^+$ $TsO^-$. Such behavior is reminiscent of that observed in related push–pull molecules.[40,41] An interpretation based on a recent theoretical account[40] is given in the Supporting Information.

**Steady-state fluorescence emission**: Most of the 5-aryl-2-pyridyloxazoles presented exhibit a strong fluorescence emission (fluorescence quantum yield, $\phi_F$, up to 0.9) in the $\lambda =$ 500–600 nm range (Figures 2b and 3b, Table 1, and the Supporting Information). This is particularly true of the 4-pyridyl series compared with the 2-pyridyl series: both states, acidic and basic, are strongly fluorescent in the former series, whereas only the basic state is noticeably fluorescent in the latter. In the emission analyses one finds, and for the same reasons, the same trends as those observed in absorption analyses: 1) a redshift upon increasing the conjugation length or by protonation of the nitrogen atom of the pyridine ring, 2) the absence of a significant influence of the substituents in the basic states, and 3) a redshift when an electron-donating group is conjugated to the pyridinium moiety (conversely, a blueshift occurs when an electron-withdrawing group is used). One notices that the oxazole substituents remote from the chromophore do not alter the photophysical features of the parent fluorophores: 4-PYMPO-$NHNH_2$, 4-PYMPO-NHNHAc, and 4-PYMPO-$NH_2$ share similar properties, as do 2-PYMPO-$CH_2OH$ and 2-PYMPO. At rather low wavelengths 4-BOMPO exhibits excellent emissive properties: both acidic and basic states are strongly fluorescent ($\phi_F = 0.65$) with maxima located at $\lambda = 442$ and 398 nm, respectively. These results can be compared with the behavior of the reported 5-(4′-dimethylaminophenyl)-2-[4-(dihydroxyboranyl)]oxazole.[21] In accordance with the weaker donor character of the methoxy group relative to that of the dimethylamino group, the emissions from both states of the methoxy derivative are strongly blueshifted with respect to those of the dimethylamino derivative (compare $\lambda = 442$ with 557 nm in the acidic state and $\lambda = 398$ with 488 nm in the basic state). In addition, whereas the fluorescence quantum yields are similar for the acidic and basic states of the methoxy compound, those of the dimethylamino compound are rather different ($\phi_F = 0.03$ for the acidic state and 0.95 for the basic state).[21] The large difference in behavior of the methoxy and the dimethylamino derivatives could reveal a difference in the nature of the emissive state. In contrast to the methoxy group, the dimethylamino substituent in the 4-position of the stilbene-4-boronic acid promotes the formation of an excited induced-charge-transfer state in polar solvents.[42]

The fluorescence emission spectra of 4-PYMPO, 4-PYMPO-$NH_2$, 2-PYMPO, and 4-PYMPOMe$^+$ $TsO^-$ were also recorded in several solvents (Table 2). They are discussed in the Supporting Information. The emission maximum ($\lambda^{(1)}_{em}$) after one-photon absorption increases with in-

  

Table 2. Solvatochromism of 4-PYMPO, 4-PYMPOMe$^+$ TsO$^-$, 2-PYMPO, and 4-PYMPO-NH$_2$. UV-visible one-photon absorption and emission features under different conditions: maxima of absorption $\lambda^{(1)}_{max}$ [nm], molar absorption coefficients $\varepsilon(\lambda^{(1)}_{max})\pm5\%$ [mM$^{-1}$cm$^{-1}$], maxima of steady-state fluorescence emission $\lambda^{(1)}_{em}$ [nm], and fluorescence quantum yields $\phi_F\pm5\%$ [%].

| Solvent ($\Delta f$[a]) | 4-PYMPO | | 4-PYMPOMe$^+$ TsO$^-$ | | 2-PYMPO | | 4-PYMPO-NH$_2$ | |
|---|---|---|---|---|---|---|---|---|
| | $\lambda^{(1)}_{max}[\varepsilon(\lambda^{(1)}_{max})]$ | $\lambda^{(1)}_{em}(\phi_F)$ | $\lambda_{max}[\varepsilon(\lambda^{(1)}_{max})]$ | $\lambda_{em}(\phi_F)$ | $\lambda^{(1)}_{max}[\varepsilon(\lambda^{(1)}_{max})]$ | $\lambda^{(1)}_{em}(\phi_F)$ | $\lambda^{(1)}_{max}[\varepsilon(\lambda^{(1)}_{max})]$ | $\lambda^{(1)}_{em}(\phi_F)$ |
| cyclohexane (−0.001) | –[b] | –[b] | –[b] | –[b] | 333[–][b] | 375(0.60) | –[b] | 373(–)[b] |
| toluene (0.013) | 335[21] | 394(0.55) | –[b] | 576(–)[b] | 330[–][b] | 389(0.55) | 330[21] | 387(0.35) |
| dioxane (0.021) | 330[–][b] | 396(0.70) | –[b] | –[b] | 330[24] | 393(0.65) | 326[26] | 403(0.20) |
| dichloromethane (0.219) | 333[22] | 415(0.60) | 427[19] | 565(0.70) | 331[23] | 404(0.55) | 330[25] | 404(0.50) |
| dimethyl sulfoxide (0.265) | 337[22] | 431(0.65) | 402[20] | 572(0.60) | 332[24] | 416(0.60) | 331[–][a] | 426(0.15) |
| acetone (0.284) | 333[20] | 417(0.55) | 403[19] | 566(0.70) | <330[–] | 404(0.40) | <330[–] | 409(0.10) |
| ethanol (0.290) | 337[19] | 433(0.80) | 411[17] | 562(0.75) | 331[–][b] | 419(0.65) | 330[26] | 422(0.15) |
| acetonitrile (0.306) | 331[22] | 423(0.70) | 403[20] | 561(0.65) | 326[20] | 411(0.60) | 327[25] | 410(0.25) |
| water (0.320) | 332[21] | 472(0.50) | 396[21] | 573(0.40) | 328[33] | 450(0.70) | 326[19] | 465(0.80) |

[a] $\Delta f=\frac{\varepsilon_r-1}{2\varepsilon_r+1}-\frac{n^2-1}{2n^2+1}$, in which $\Delta f$ is the orientation polarizability and $\varepsilon_r$ is the dielectric constant.[2] [b] The solubility was too low to derive reliable data.

creasing solvent polarity for the basic states (4-PYMPO, 4-PYMPO-NH$_2$, and 2-PYMPO); in contrast, $\lambda^{(1)}_{em}$ of 4-PYMPOMe$^+$ TsO$^-$ is not significantly sensitive to the solvent polarity. Similar observations were made in related push–pull molecules.[40,41]

**Two-photon absorption**: A series of experiments was undertaken to evaluate the typical magnitude of the cross sections for two-photon absorption of the present 5-aryl-2-pyridyloxazoles. We retained the molecules that showed significant one-photon absorption above $\lambda=350$ nm and that were strongly fluorescent. Figures 2a and 3a display typical examples of the two-photon excitation spectra observed for the basic and acidic states of the corresponding oxazoles at 298 K (also see the Supporting Information). They were recorded with a homebuilt setup[43] using the reported excitation spectrum of fluorescein for calibration.[22] For all the investigated compounds, the power-squared dependence of two-photon excitation fluorescence was checked at several wavelengths in the investigated range and revealed satisfactory behavior over the 0–60 mW range. The two-photon absorption spectra compare well with the one-photon absorption spectra after dividing the wavelength by a factor 2 (Table 1). This suggests that the same excited states are reached regardless of the excitation mode. Such an observation is in agreement with other reports making use of a comparable technique on unsymmetrical donor–acceptor compounds.[22,43] A typical order of magnitude of the peak two-photon absorptivities in the present series is 40–80$\pm$10 GM (1 GM$=10^{-50}$ cm$^4$s(photon-molecule)$^{-1}$). Taking into account the large fluorescence quantum yields, such values of the two-photon absorptivities compare well with the corresponding values for commonly employed pH probes (fluorescein at pH 11: $\delta^{(2)}_{max}(780\text{ nm})=35$ GM, $\phi_F=0.9$; pyranin backbone: $\delta^{(2)}_{max}(750\text{ nm})=4$ GM, $\phi_F=0.54$[44]). In fact, they can be observed for the protonated states because the corresponding maxima lie within the accessible range of the investigated wavelengths ($\lambda^{(2)}=700$–900 nm). In contrast, the two-photon excitation spectra of the basic states were blue-shifted and lower values of the two-photon absorptivities were observed at the lowest excitation wavelength ($\lambda^{(2)}=$ 700 nm). Similar alterations to the two-photon excitation spectra have already been observed either upon protonation[45] or upon interaction with metal cations.[46,47]

## Acidobasic properties

*Absorption measurements*: Figure 4a displays a typical evolution of the absorption spectra after one-photon excitation

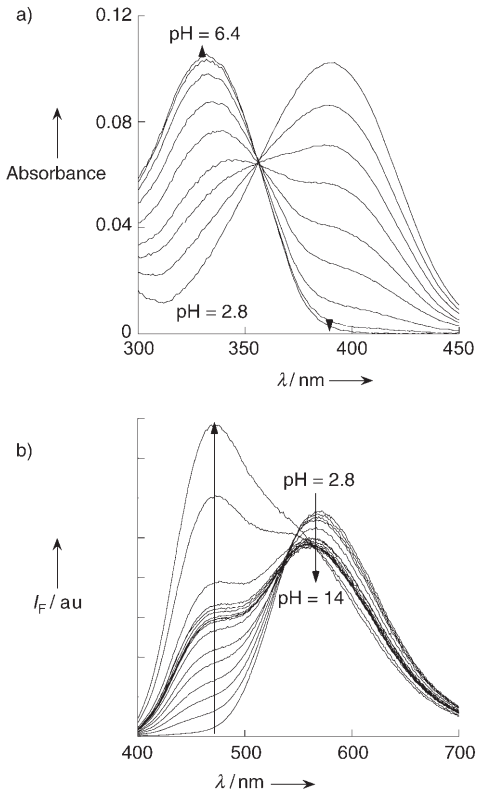


Figure 4. Dependence on pH of a) the absorption (from acidic to basic conditions: pH 2.8, 3.7, 4.0, 4.3, 4.6, 4.8, 5.3, 5.9, 6.4) and b) the emission (from acidic to basic conditions: pH 2.8, 3.7, 4.0, 4.3, 4.6, 4.8, 5.3, 5.9, 6.4, 6.8, 7.5, 8.5, 9.2, 10.7, 12.5, 13.2, 14.0) spectra of 4-PYMPO after one-photon excitation ($\lambda^{(1)}_{exc}=339$ nm, [4-PYMPO]$=5$ μM). Solvent: Britton–Robinson buffer[53] (0.1 M) at 293 K.

  

in the present oxazole series. Except for the two acidic 5-aryl-2-pyridiniumoxazoles (2-PYMPOH$^+$-$CO_2$H and 2-PYMPOH$^+$-$CO_2$Me) and the polyacids (4-PYMPOH$^+$-$NHNH_3^+$, 4-PYHPOH$^+$, and 2-PYMPOH$^+$-$CO_2$H), these evolutions are satisfactorily accounted for by a one-proton exchange reaction [Eq. (1)] in the investigated pH range:

$$B + H_2O = BH^+ + OH^- \quad (1)$$

in which $BH^+$ and B stand for the acidic and the basic states of the pH probe, respectively. These evolutions can be analyzed to derive the $pK_a(BH^+/B)$ of the protonated ground states (see the Supporting Information). In all the investigated cases, the extracted $pK_a$ values confirm the observations from the photophysical studies, that is, protonation occurs at the nitrogen atom of the pyridine ring. The $pK_a$ shifts observed by adding substituents on the pyridine ring are similar in the present oxazole series and in the pyridine series.[23] Furthermore, one anticipates much lower $pK_a$ values for acids that result from the protonation of the nitrogen atom of the oxazole ring ($pK \simeq 0$).[23]

The relationship between the structure of the pyridinium moiety of the present oxazoles and the $pK_a(BH^+/B)$ value is displayed in Table 3. As a general rule, the $pK_a$ values of the 2-pyridyl series are lower than those of the 4-pyridyl series. This observation may result from the larger steric hindrance of the 2-pyridyl series in the acidic state. Remote substituents do not alter acid–base properties: 4-PYPO, 4-PYMPO, and 4-PYHPO share the same $pK_a$ value. Substituent effects are generally more important at the level of the pyridine ring. In accordance with the absence of a significant electronic difference, 2-PYMPO and 2-QUIMPO exhibit similar $pK_a$ values. The $pK_a$ of 2-PYMPO-$CH_2$OH is lower than those of the preceding compounds; this observation could originate from the steric hindrance altering the nitrogen environment and/or from the possible formation of a hydrogen bond between the nitrogen lone pair and the nearby hydroxyl group. The electron-donating groups generally increase the $pK_a$ when they are conjugated to the nitrogen atom of the pyridine ring: 4-PYMPOM, 4-PYMPO-$NHNH_2$, and 4-PYMPO-$NH_2$ possess significantly larger $pK_a$ values than that of 4-PYMPO. In contrast, the electron-withdrawing groups lower the $pK_a$. In the case of 2-PYMPO-$CO_2$H and 2-PYMPO-$CO_2$Me, the $pK_a$ is less than 1; this is the lowest limit that we investigated during the present series of experiments.

UV-visible absorption spectroscopy was also used to measure the $pK_a$ values of the polyacids: $pK_a$(4-PYMPO-$NHNH_3^+$/4-PYMPO-$NHNH_2$) = 10.5, $pK_a$(4-PYHPO/4-$PYPO^-$) = 8.1, and $pK_a$(2-PYMPO-$CO_2$H/2-PYMPO-$CO_2^-$) = 3.5, which agree well with typical values for the corresponding acidic groups.[23]

In the case of 4-BOMPO, we found $pK_a$(4-BOMPO/4-BOMPO$(OH)^-$) = 8.1, which is in good agreement with the value that was reported for the dimethylamino derivative ($pK_a$ = 7.8).[21]

Table 3. $pK_a$ of the pyridine moiety of the oxazole derivatives: $pK_a^{abs}(BH^+/B)$ as measured by UV-visible absorption, $pK_a^{em}(BH^+/B)$, and $pK_a^{em}(BH^{+*}/B^*)$ as measured from fluorescence emission, and $pK_a^{spec}(BH^{+*}/B^*)$, as evaluated from Equation (3) in Britton–Robinson buffer[53] (0.1 M) at 293 K.

| B | $pK_a^{abs}(BH^+/B) \pm 0.1$ | $pK_a^{em}(BH^+/B) \pm 0.1$ | $pK_a^{em}(BH^{+*}/B^*)$ | $pK_a^{spec}(BH^{+*}/B^*)$ |
|---|---|---|---|---|
| 4-PYPO | 4.3 | 4.3 | –[a] | 12.4 |
| 4-PYMPO | 4.3 | 4.4 | 14.1 ± 0.4 | 12.7 |
| 4-PYMPOM | 5.7 | –[a] | –[a] | 13.3 |
| 2-PYMPO | 2.6 | 2.8 | 9 ± 1 | 11.6 |
| 2-QUIMPO | 2.2 | 2.9 | 8 ± 1 | 10.4 |
| 4-PYMPO-$NHNH_2$[b] | 5.4 | 6.1 | – | 7.7 |
| 4-PYMPO-NHNHAc[c] | – | 4.0 | – | 10.6 |
| 4-PYMPO-$NH_2$ | 5.7 | 5.7 | – | 11.0 |
| 4-PYHPO[d] | 4.3 | – | – | 12.4 |
| 2-PYMPO-$CO_2$H | –[a] | –[a] | –[e] | – |
| 2-PYMPO-$CO_2$Me | –[a] | –[a] | 3.8 ± 0.3 | – |
| 2-PYMPO-$CH_2$OH | 1.8 | 2.4 | 9 ± 1 | 11.0 |
| 4-BOMPO | 8.1 | 8.0 | – | 11.6 |

[a] Not determined. [b] This is a dibase. The values given refer to the couple 4-PYMPOH$^+$-$NHNH_3^+$/4-PYMPO-$NHNH_3^+$ involving the nitrogen atom of the pyridine ring. The second $pK_a$ corresponding to the couple 4-PYMPO-$NHNH_3^+$/4-PYMPO-$NHNH_2$ was found equal to 10.5 by UV absorption and to 11.4 by fluorescence emission. [c] This is not very soluble in basic aqueous solutions. We extracted $pK_a$ = 3.6 from the UV-visible titration but we are less confident in this value than in that extracted from fluorometry. [d] 4-PYHPOH$^+$ is a diacid. The values given refer to the couple 4-PYHPOH$^+$/4-PYHPO involving the nitrogen atom of the pyridine ring. The second $pK_a$ corresponding to the couple 4-PYHPO/4-$PYPO^-$ was found equal to 8.1 by UV absorption. [e] 2-PYMPOH$^+$-$CO_2$H is a diacid. From the consideration of the wavelengths of absorption and emission, we tentatively assume that no measured values refer to the deprotonation of the nitrogen atom of the pyridine ring. In contrast, the first observed $pK_a$ corresponds to the couple 2-PYMPO-$CO_2$H/2-PYMPO-$CO_2^-$ and is equal to 3.5 by UV absorption, and 3.2 by fluorescence emission. In addition, we observed by fluorescence emission a second $pK_a$ = 6.9 that we tentatively attribute to the deprotonation of the excited state 2-PYMPO-$CO_2$H*.

*Steady-state fluorescence measurements*: The dependence of the emission spectrum as a function of pH is more difficult to analyze in the present series. As an example, Figure 4b displays the evolution of the emission spectrum of 4-PYMPO when the pH is increased. Figure 5a additionally displays the ratio ($\rho^{e,(1)}_{472/569}$) of the 4-PYMPO fluorescence intensities at $\lambda$ = 472 and 569 nm when the one-photon excitation is performed at the isosbestic point (see the Supporting Information). Below $pK_a$(4-PYMPOH$^+$/4-PYMPO) = 4.3, determined from UV-visible absorption spectroscopy, one observes the emission from the protonated excited state 4-PYMPOH$^{+*}$. Around pH = $pK_a$ the band associated with the emission from 4-PYMPOH$^{+*}$ drops, while a new band that corresponds to emission from the basic excited state 4-PYMPO* appears. Nev-

  

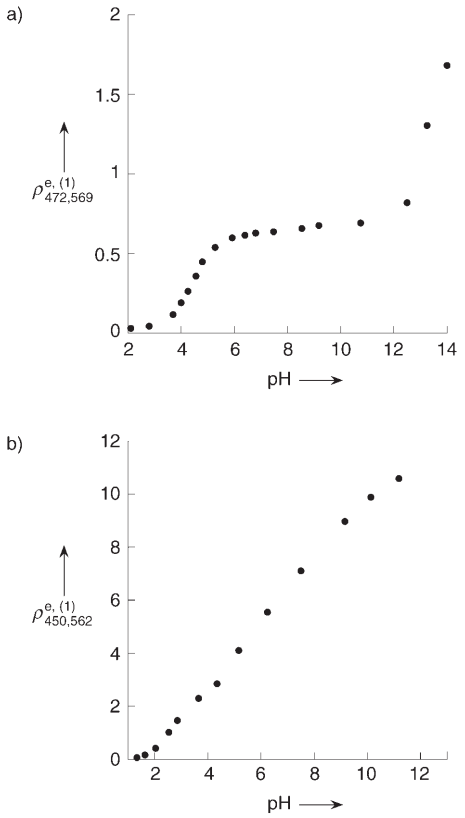


Figure 5. Evolution of the ratio ($\rho^{e,(1)}_{\lambda_1\lambda_2}$) of the fluorescence emissions at $\lambda_1$ and at $\lambda_2$ after one-photon excitation. a) 4-PYMPO: $\lambda_1=472$, $\lambda_2=569$, $\lambda_{exc}=339$ nm; b) 2-PYMPO: $\lambda_1=450$, $\lambda_2=562$, $\lambda_{exc}=338$ nm. Solvent: Britton–Robinson buffer[53] (0.1 M) at 293 K.

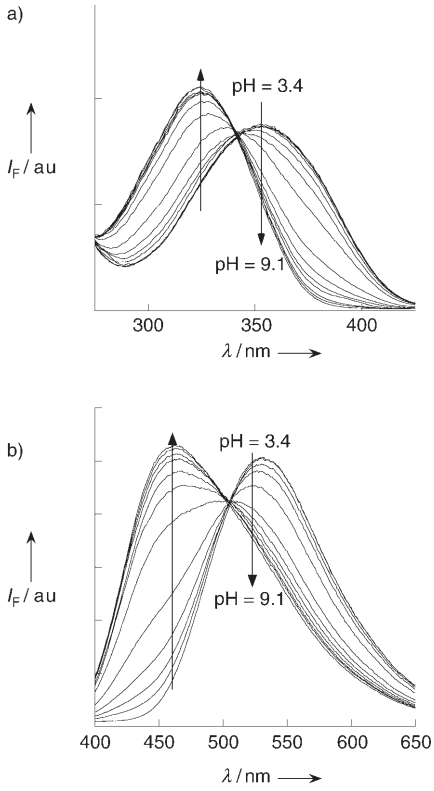


Figure 6. Dependence on pH of the excitation (a) and of the emission spectra (b); adapted from ref. [13]) of 4-PYMPO-$NH_2$ (from acidic to basic: pH 3.4, 4.5, 4.8, 5.1, 5.5, 6.0, 6.2, 6.5, 6.7, 7.0, 7.3, 9.1). [4-PYMPO-$NH_2$] = 100 nM. Solvent: Britton–Robinson buffer[53] (0.1 M) at 293 K.

ertheless, the emission band of 4-PYMPOH$^+$* persists even beyond the p$K_a$ value. In fact, the emission spectrum from the solution of 4-PYMPO essentially remains unchanged in the pH 6–9 range. It is only beyond pH 13 that one observes the gradual disappearance of the emission originating from 4-PYMPOH$^+$* and the evolution towards the emission spectrum of 4-PYMPO* alone.

In addition to 4-PYMPO, five members of the present series exhibit this "abnormal" behavior under our experimental conditions: 4-PYMPOM, 2-PYMPO, 2-QUIMPO, 2-PYMPO-$CO_2$Me, and 2-PYMPO-$CH_2$OH. For example, Figure 5b displays the unexpected dependence on pH of the ratio $\rho^{e,(1)}_{450/562}$ of the fluorescence emissions at $\lambda=450$ and at 562 nm for 2-PYMPO when the one-photon excitation is performed at the isosbestic point. Instead of a classical threshold over 2–3 pH units (see Figure 9 later for an example), one observes a continuous evolution over 10 pH units! In contrast, Figure 6 displays the evolution of pH of the fluorescence excitation and fluorescence emission spectra of 4-PYMPO-$NH_2$. They exhibit the "normal" trend expected for a compound with only one p$K_a$.

*Time-resolved fluorescence measurements*: We envisaged that the preceding "abnormal" behavior could result from a large increase of 4-PYMPO basicity upon excitation.[14–16,48] Figure 7a and b display the different reactions that occur when a solution containing two bases, B (here the fluorophore, in its ground or excited state) and Y (for instance, the basic state of the buffer), is illuminated. Under appropriate kinetic conditions, protonation of the basic excited state (4-PYMPO*) can take place during its lifetime. Then one would observe the fluorescence emission from the acidic excited state (4-PYMPOH$^+$*) even above the p$K_a$(4-PYMPOH$^+$/4-PYMPO) associated with the ground state. To evaluate the latter assumption, we performed time-resolved fluorescence measurements with solutions of 4-PYMPO at different pH. The results are displayed in Figure 8 and Table 4. Three different pH domains emerge from consideration of Table 4: pH $\leq$ 3, 3 < pH < 14, and pH > 14.

At pH $\leq$ 3, most of the ground-state molecules present in solution are protonated. Upon excitation, these 4-PYMPOH$^+$ molecules become excited 4-PYMPOH$^+$* molecules, as shown in the set of reactions displayed in Figure 7a and b. In relation to fluorescence emission, the question arises as to whether some basic excited state 4-PYMPO* can form during the lifetime $\tau_{(4\text{-PYMPOH}^{+*})}$ of the acidic excited state 4-PYMPOH$^+$*. Three reactive channels have to be considered (Figure 7a and b): 1*3* (reaction of 4-PYMPOH$^+$* with $H_2O$), 2*3* (reaction of 4-PYMPOH$^+$* with $OH^-$), and 3′*3* (reaction of 4-PYMPOH$^+$* with the

  

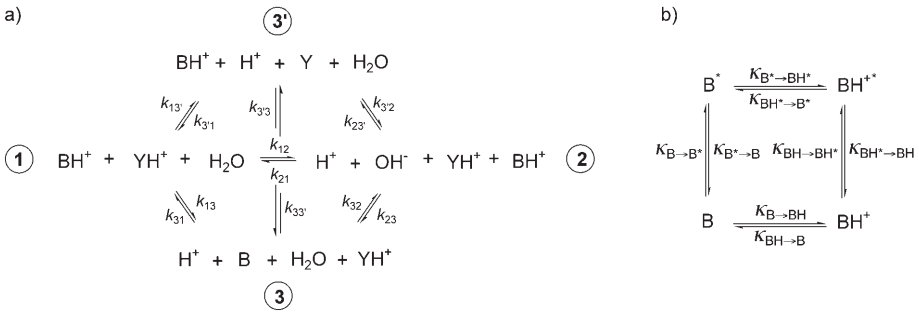


Figure 7. a) Reactions involved in the mechanism of dissociation/recombination of an acid–base couple $BH^+/B$ in aqueous solution in the presence of another acid–base couple $YH^+/Y$. b) Interconversion processes between the acidic and basic forms of the $BH^+/B$ couple in the ground and excited states. The subscript of the rate constant refers to the exchange processes that are displayed in a) (a star means that an excited state is considered), and the notation $\kappa$ corresponds to the sum of all the pseudo first-order rate constants that are involved in any exchange process that is shown in a): $k_{(BH\rightarrow B)}=k_{13}+k_{23}OH+k_{3'3}Y$; $\kappa_{(B\rightarrow BH)}=k_{31}H+k_{32}+k_{33'}YH$; $\kappa_{(BH\rightarrow BH^*)}=\frac{2.3\varepsilon_{BH}(\lambda_{exc})lI_0(\lambda_{exc})}{V}$ with one-photon excitation; whereas, $\kappa_{(BH\rightarrow BH^*)}=\frac{\delta_{BH}(\lambda_{exc})I_0^2(\lambda_{exc})}{2S^2}$ with two-photon excitation; $\kappa_{(BH^*\rightarrow BH)}=\frac{1}{\tau_{BH^*}}$; $\kappa_{(BH^*\rightarrow B^*)}=k_{13}^*+k_{23}^*OH+k_{3'3}^*Y$; $\kappa_{(B^*\rightarrow BH^*)}=k_{31}^*H+k_{32}^*+k_{33'}^*YH$; $k_{(B\rightarrow B^*)}=\frac{2.3\varepsilon_B(\lambda_{exc})lI_0(\lambda_{exc})}{V}$ with one-photon excitation, whereas $\kappa_{(B\rightarrow B^*)}=\frac{\delta_A(\lambda_{exc})I_0^2(\lambda_{exc})}{2S^2}$ with two-photon excitation; $\kappa_{(B^*\rightarrow B)}=\frac{1}{\tau_{B^*}}$, in which $k_{ij}$ = rate constant associated with the reaction $i\rightarrow j$; $\varepsilon(\lambda_{exc}^{(1)})$and $\delta(\lambda_{exc}^{(2)})$ = molar absorption coefficient and cross section for two-photon absorption at the excitation wavelength, respectively; $l$ = length of the light pathway in the sample; $S$ = surface of the light beam; $V$ = volume of irradiated sample; $I_0$ = intensity of the incident light at the excitation wavelength; $\tau$ = lifetime of the excited state. For clarity, brackets and charges have been omitted from the concentration notation.

basic state, Y, of the buffer). Under the present experimental conditions, channel 2*3* is the fastest, but $k_{2*3*}OH < 10^{-1}\,s^{-1}$ remains much lower than $\frac{1}{\tau_{(4\text{-}PYMPOH^{+}*)}}\approx 10^9\,s^{-1}$ (see below); therefore, 4-$PYMPOH^{+}$* deprotonation cannot occur during its lifetime. In principle, one should observe only the emission from 4-$PYMPOH^{+}$* at any pH below 3. Indeed, upon excitation at $\lambda = 360$ nm, one observes that the decay of fluorescence emission from the solution is monoexponential. Nevertheless, one also notices that the extracted lifetime drops as the pH is lowered. In addition to the decrease of intensity of steady-state fluorescence emission from 4-$PYMPOH^{+}$* at low pH (data not shown in Figure 4b), this observation suggests that a poorly fluorescent complex, 4-$PYMPOH_2^{2+}$*, forms between the 4-$PYMPOH^{+}$* excited state and the proton (dynamic quenching). In fact, the formation of a complex between the 4-$PYMPOH^{+}$ ground state and the proton (static inhibition) can be excluded on the basis of the dependence of the fluorescence lifetime on pH and of the absence of any evolution of the absorption spectrum below pH 3. The intrinsic lifetime of the excited acidic state 4-$PYMPOH^{+}$* and the rate constant for dynamic quenching by the proton ($k_Q$) were derived from a Stern–Volmer analysis of the lifetimes given in Table 4 below pH 3 (see the Supporting Information). We found that $\tau_{(4\text{-}PYMPOH^{+}*)}=1.5\pm 0.1$ ns and $k_Q=0.9\pm0.1\times10^{10}\,M^{-1}s^{-1}$. The latter value suggests that quenching by the proton is controlled by diffusion.[25] This quenching might be associated with the protonation of the nitrogen atom of the oxazole ring in the excited state.

At pH > 14, there are ground-state 4-PYMPO molecules in solution. Upon excitation, they give excited 4-PYMPO*

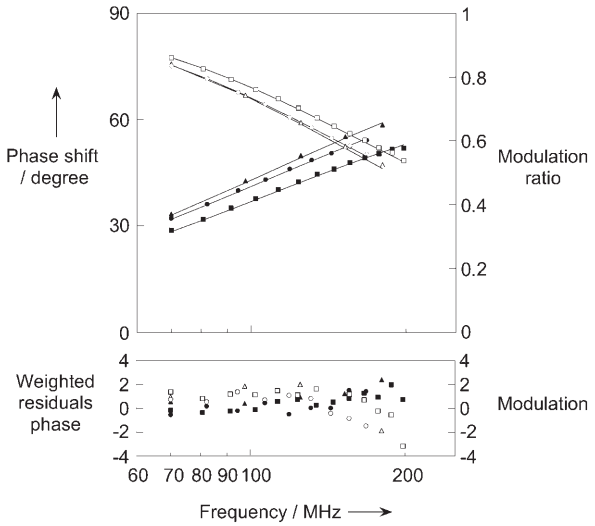


Figure 8. Phase shifts (filled markers) and modulation ratios (empty markers) versus frequency for 4-PYMPO at different pH values. pH 3: triangles; pH 4: circles; pH 5: squares; Solvent: Britton–Robinson buffer[53] (0.1 M) at 293 K.

Table 4. Dependence on pH of the rate constants for relaxation of the 4-PYMPO excited state in aqueous solution as extracted from the data collected by phase-modulation fluorometry at 298 K [see Eq. (6)].[a]

| pH | $f_{1,pH}$ | $\frac{1}{\beta_{1,pH}}\pm0.1$ [ns] | $f_{2,pH}$ | $\frac{1}{\beta_{2,pH}}\pm0.05$ [ns] | $\chi^2\pm0.1$ | $a_{1,pH}$ | $a_{2,pH}$ |
|---|---|---|---|---|---|---|---|
| 1.0 | 1.00 | 0.6 | – | – | 1.9 | 1.00 | 0.00 |
| 1.6 | 1.00 | 1.1 | – | – | 1.5 | 1.00 | 0.00 |
| 2.0 | 1.00 | 1.3 | – | – | 0.9 | 1.00 | 0.00 |
| 2.6 | 1.00 | 1.4 | – | – | 0.5 | 1.00 | 0.00 |
| 3.0 | 1.00 | 1.5 | – | – | 2.3 | 1.00 | 0.00 |
| 4.0 | 0.83 | 1.6 | 0.17 | 0.30 | 1.2 | 0.71 | 0.29 |
| 5.0 | 0.84 | 1.4 | 0.16 | 0.45 | 1.2 | 0.63 | 0.37 |
| 6.0 | 0.81 | 1.4 | 0.19 | 0.45 | 1.0 | 0.59 | 0.41 |
| 8.0 | 0.81 | 1.4 | 0.19 | 0.45 | 1.0 | 0.59 | 0.41 |
| 8.0[b] | 1.36 | 1.5 | −0.36 | 0.45 | 0.95 | 0.54 | −0.46 |
| 9.0 | 0.83 | 1.4 | 0.17 | 0.45 | 1.1 | 0.60 | 0.40 |
| 10.0 | 0.80 | 1.5 | 0.20 | 0.50 | 1.1 | 0.59 | 0.41 |
| 12.0 | 0.82 | 1.5 | 0.18 | 0.45 | 1.9 | 0.58 | 0.42 |
| 13.0 | 0.91 | 1.7 | 0.09 | 0.30 | 1.4 | 0.65 | 0.35 |
| 14.0 | 0.96 | 2.0 | 0.04 | 0.25 | 1.3 | 0.74 | 0.26 |
| > 14 | 1.00 | 2.7 | – | – | 0.7 | 1.00 | 0.00 |

[a] $\frac{1}{\beta_{1,pH}}$, $\frac{1}{\beta_{2,pH}}$ = monoexponential decay of fluorescence emission of components 1 and 2, respectively; $\chi$ = mean square deviation. [b] Selective observation of the acidic state of 4-PYMPO.

molecules that react as displayed in Figure 7a and b. As described in the preceding paragraph, the question arises as to whether some acidic excited state 4-PYMPOH$^+$* can form during the lifetime of the basic excited state 4-PYMPO*. Three reactive channels have again to be considered: 3*1* (reaction of 4-PYMPO* with $H^+$), 3*2* (reaction of 4-PYMPO* with $H_2O$), and 3*3′* (reaction of 4-PYMPO* with the acidic state $YH^+$ of the buffer). The fastest channel is 3*2* with a $k_{3*2*}$ value that is larger than $\frac{1}{\tau_{(4\text{-PYMPO}*)}} \approx 10^9\ s^{-1}$ (see below): at the $\tau_{(4\text{-PYMPO}*)}$ timescale, chemical relaxation can now occur leading to the formation of the most stable species in the excited state. The latter is 4-PYMPO* if $pK_a$(4-PYMPOH$^+$*/4-PYMPO*) $\leq 14$. Under such conditions, one expects to observe the fluorescence emission from 4-PYMPO* only. Indeed, upon excitation at $\lambda = 360$ nm, a monoexponential decay of fluorescence emission attributed to 4-PYMPO* was observed: $\tau_{(4\text{-PYMPO}*)} = 2.7 \pm 0.1$ ns (Table 4).

The analysis is more intricate for $4 < pH < 14$. Above $pK_a$(4-PYMPOH$^+$/4-PYMPO) = 4.3, the solution essentially contains the basic ground state 4-PYMPO. Nevertheless, one observes that the fluorescence emission from the solution now contains two contributions. The first arises from the basic excited state 4-PYMPO*, whereas the second originates from the acidic, protonated excited state 4-PYMPOH$^+$* that is formed during the lifetime of 4-PYMPO*. This interpretation is strengthened by the results of the experiment performed at pH 8 when one observes emission from the acidic excited state 4-PYMPOH$^+$* only. The decay behavior is in agreement with the prediction given in the Supporting Information [Eq. (31)]: $a_1 \approx -a_2$, in which $a$ is the pH-dependent amplitude associated with the lifetime of the component (1 or 2) being measured.

For $4 < pH < 14$, the relative populations in the excited state are under kinetic control and depend on many parameters (see above). By taking into account the measured intrinsic lifetime of 4-PYMPO* and 4-PYMPOH$^+$*, one experimentally obtains the values of the rate constants $\kappa_{(4\text{-PYMPO}*\rightarrow 4\text{-PYMPOH}*)}$ and $\kappa_{(4\text{-PYMPOH}*\rightarrow 4\text{-PYMPO}*)}$ associated with the 4-PYMPO* protonation and the 4-PYMPOH$^+$* deprotonation, respectively (see above). Both $\kappa_{(4\text{-PYMPO}*\rightarrow 4\text{-PYMPOH}*)}$ and $\kappa_{(4\text{-PYMPOH}*\rightarrow 4\text{-PYMPO}*)}$ contain three contributions: 3*1*, 3*2*, and 3*3′* on the one hand, and 1*3*, 2*3*, and 3′*3* on the other. Now the problem is to evaluate the significant individual rate constants from investigating the dependence of $\kappa_{(4\text{-PYMPO}*\rightarrow 4\text{-PYMPOH}*)}$ and $\kappa_{(4\text{-PYMPOH}*\rightarrow 4\text{-PYMPO}*)}$ on pH. To facilitate the analysis, we successively considered reduced pH domains in which one (or two) individual rate constant(s) dominate(s) the whole behavior.

At $4 < pH < 12$, 4-PYMPO* protonation is governed by the reactions with water and with the protonated state of the buffer. Linear fitting of $\kappa_{(4\text{-PYMPO}*\rightarrow 4\text{-PYMPOH}*)}$ as a function of the concentration in $YH^+$[49] provides $k_{3*2*} = 1.4 \pm 0.5 \times 10^9\ s^{-1}$ and $k_{3*3'*} = 1.8 \pm 0.6 \times 10^{10}\ M^{-1}s^{-1}$. For $13 < pH < 14$, 4-PYMPO* protonation is only controlled by reaction with water; $k_{2*3*}$ and $k_{3*2*}$ are directly derived from the experiments. We found that $k_{2*3*} = 1.7 \pm 0.3 \times 10^9\ M^{-1}s^{-1}$ and $k_{3*2*} = 1.8 \pm 0.7 \times 10^9\ s^{-1}$. From the whole series of experiments, we obtain $k_{2*3*} = 1.5 \pm 0.5 \times 10^9\ M^{-1}s^{-1}$ and $k_{3*2*} = 1.8 \pm 0.7 \times 10^9\ s^{-1}$. From this one can derive $pK_a$(4-PYMPOH$^+$*/4-PYMPO*) $= -\log(K_e \frac{k_{2*3*}}{k_{3*2*}}) = 14.1 \pm 0.4$ in which $K_e$ designates the ionization constant of water at room temperature: the $pK_a$ of 4-PYMPOH$^+$ is shifted by 10 pH units upon light excitation! In addition, the $k_{2*3*}$ value is in line with the corresponding value for imidazole in its ground state (the pyridine value was not measured in ref. [25]) at $k_{23} = 2.5 \times 10^{10}\ M^{-1}s^{-1}$.[25] The lowest value observed for $k_{2*3*}$ is in agreement with the much smaller difference between the involved $pK_a$ in our case: $pK_a(H_2O/OH^-) - pK_a$(4-PYMPOH$^+$*/4-PYMPO*) $\approx 0$ whereas $pK_a(H_2O/OH^-) - pK_a(BH^+/B) \approx 7$ in the case of imidazole.[25]

*Dual-emission-wavelength measurements*: In a ratiometric measurement based on a pH probe exchanging between an acidic (A) and a basic (B) state, the absorbance or the emission intensity, here denoted $I^{abs/em}$, is recorded at two different wavelengths, $\lambda_1$ and $\lambda_2$. Then the pH is extracted from the ratio $R(pH) = \frac{I_{\lambda_1}^{abs/em}}{I_{\lambda_2}^{abs/em}}$ by using Equation (2):[2]

$$pH = pK_a + \log\frac{R - R_A}{R_B - R} + \log\frac{I_{\lambda_2}^{abs/em}(A)}{I_{\lambda_2}^{abs/em}(B)} \qquad (2)$$

in which the $pK_a$ values designate the protonation constant of the couple (A,B), $R_A$ and $R_B$ are the values of the ratio measured at $\lambda_1$ and $\lambda_2$ on the spectra recorded from solutions containing A or B only, and $\frac{I_{\lambda_2}^{abs/em}(A)}{I_{\lambda_2}^{abs/em}(B)}$ is the value of the ratio of the signals at $\lambda_2$ from solutions containing either A or B at the same concentration.

When the ratiometric pH measurement relies on absorption, the $pK_a$ in Equation (2) is the protonation constant of the ground state, $pK_a(BH^+/B)$, and $R_{BH+}$, $R_B$, $I_{\lambda_2}^{abs}(BH^+)$, and $I_{\lambda_2}^{abs}(B)$ are simply extracted from the absorption spectra recorded below $pK_a(BH^+/B) - 2$ and above $pK_a(BH^+/B) + 2$. In contrast, in the case of a ratiometric pH measurement based on fluorescence emission, proton-exchange reactions may occur in the excited state. Under such conditions, the concentrations in excited states that do emit fluorescence do not simply reflect the corresponding concentrations in the ground state [Eqs. (10) and (11) in the Supporting Information]. Following this, the values of $R$ and $I_{\lambda_2}^{abs/em}$ below $pK_a(BH^+/B) - 2$ and above $pK_a(BH^+/B) + 2$ may not be easily related to the values intrinsic to $BH^+$ and B anymore: $R_{BH+}$, $R_B$, $I_{\lambda_2}^{em}(BH^+)$, and $I_{\lambda_2}^{em}(B)$. As shown in the general expression of the ratio measured at $\lambda_1$ and $\lambda_2$ [Eq. (25) in the Supporting Information], ratiometric pH measurements now require either careful calibration under controlled conditions, or complementary measurements such as lifetimes and rate constants for proton exchange. In particular, in the absence of any relevant information about the concentration and the nature of the buffer (in biological systems for instance), one cannot predict the evolution of the emission spectrum as a function of pH.

  

As a significant example, the "abnormal" behavior observed in Figure 5b results from controlling the protonation of the excited basic 2-PYMPO* state by using pH-dependent amounts of protonated species derived from the three-component buffer: the larger the amount, the larger the extent of formation of the protonated excited state 2-PYMPOH$^+$*. In fact, here one observes the titration curve of the buffer between p$K_a$(BH$^+$/B) and p$K_a$(BH$^+$*/B*)!

In contrast, 4-PYMPO-NH$_2$ and its closely related derivatives seem to be appropriate for multiple ratiometric pH measurements because they exhibit the "normal" trend expected for a compound with only one p$K_a$ in absorption and in emission (see Figure 6). In particular, Figure 9 suggests

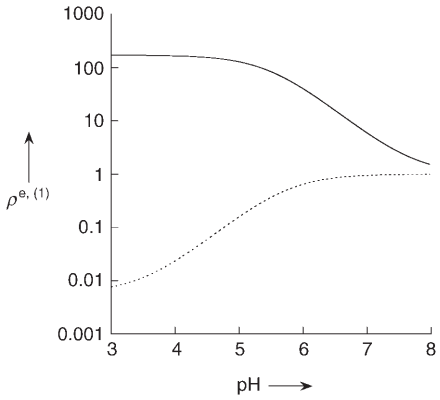


Figure 9. Evolution of the ratio $\rho^{e,(1)}$ of the fluorescence emissions at two different wavelengths from a solution of 4-PYMPO-NH$_2$ after one-photon excitation. Solid line: $\rho^{e,(1)}_{600/400}$, $\lambda^{(1)}_{exc}=395$ nm; Dotted line: $\rho^{e,(1)}_{400/600}$, $\lambda^{(1)}_{exc}=300$ nm. The curves were calculated with Equation (2) by using the parameter values measured during the present study. [4-PYMPO-NH$_2$]= 100 nM. Solvent: Britton–Robinson buffer[53] (0.1 M) at 293 K.

that 4-PYMPO-NH$_2$ could be used as a fluorescent probe to measure pH by any ratiometric method based on fluorescence emission in the pH 3–8 range by tuning both the excitation and the emission wavelengths. When the one-photon excitation favors the acidic state ($\lambda^{(1)}_{exc}=395$ nm), the ratio $\rho^{e,(1)}_{600/400}$ of the fluorescence emissions at $\lambda=600$ and at 400 nm varies by two orders of magnitude in the pH 5.5–7.5 range. A similar amplitude is observed for $\rho^{e,(1)}_{400/600}$ in the pH 3.5–5.5 range in which the excitation now favors the basic state ($\lambda^{(1)}_{exc}=300$ nm).

## Discussion

The present study emphasizes that the design of a fluorescent pH probe relying on a ratiometric analysis of the fluorescence emission is a delicate task. The introduction on a donor–acceptor backbone of an electron-donating or -accepting group that exhibits acid–base properties is a natural choice to strongly shift the absorption/emission from the acidic and the basic states of the indicator. At the same time, some difficulty may originate from the possible change of the p$K_a$ of the pH probe upon light absorption. Thus, pH can be ratiometrically measured by applying Equation (2) to the absorption or fluorescence excitation spectra of any of the oxazoles. Attractive photophysical features and a broad p$K_a$ range enable the easy measurement of pH over a large domain. In contrast, the protonation occurring during the lifetimes of the excited basic state of most present fluorescent pH probes hinders ratiometric pH measurements based on fluorescence emission. The following discussion attempts to analyze the singular behavior of 4-PYMPO-NH$_2$ and its derivatives in the oxazole series.

We first focus on the lifetime of the B* states in the whole series of oxazoles (BH$^+$/B) investigated in the present study. Indeed, the latter factor controls the width of the kinetic window during which any protonation can take place in the excited state. Time-resolved experiments on solutions of 4-PYMPO gave lifetimes in the nanosecond range for 4-PYMPOH$^+$* and 4-PYMPO*. We did not perform extensive determinations of the lifetimes of the basic excited states of the other oxazoles. In fact, the similarity of their molar absorption coefficients and of their maxima of absorption suggest that the rate constants for radiative deactivation $S_1 \rightarrow S_0$ with fluorescence emission ($k_r$) should remain in the same range within the series.[50] Following this, the lifetimes of the basic excited states should lie in the same nanosecond range for all of the investigated compounds in view of the uniformity of their large fluorescence quantum yields in the whole series as $k_r=\frac{\phi}{\tau}$.[2] Hence 4-PYMPO-NH$_2$ singularity should not originate from its lifetime.

One is then left to examine whether the 4-PYMPO-NH$_2$ singularity could be linked to the absence of a p$K_a$ shift upon light absorption (thermodynamic control) or to the protonation during the lifetime of the basic excited state being too slow (kinetic control). To address the corresponding issue, we evaluated the protonation constant of the excited state by using Equation (3):

$$2.3k_BT[pK_a(BH^{+}*/B^*)-pK_a(BH^+/B)] = hc\left(\frac{1}{\lambda_{abs}(B)}-\frac{1}{\lambda_{abs}(BH^+)}\right)+\frac{1}{2}[S(BH^+)-S(B)] \quad (3)$$

in which $k_B$ is the Boltzmann constant, $T$ is the absolute temperature, $h$ is the Planck constant, $c$ is the light velocity, and $S$(BH$^+$) and $S$(B) are the experimental Stokes shifts for BH$^+$ and B, respectively. Equation (3) results from the Förster cycle,[2] or from a more elaborate theory that explicitly takes into account the reorganization energies of the solvent[40] under assumptions given in the Supporting Information. Table 2 displays the estimates of p$K_a^{spec}$(BH$^+$*/B*) obtained from Equation (3) by using the p$K_a$(BH$^+$/B) values obtained from UV-visible absorption measurements. In the case of 4-PYMPO*, the comparison between the p$K_a^{spec}$ estimate and the p$K_a^{em}$ value extracted from time-resolved measurements gives an order of magnitude of the uncertain-

  

ty associated with using Equation (3) to evaluate the protonation constants in the excited state: $pK_a^{em}$ is larger than $pK_a^{spec}$ by 1.4 pH units. Despite this limitation, the main result from the derivation of the $pK_a^{spec}(BH^{+}*/B*)$ value is that $pK_a(BH^{+}*/B*)-pK_a(BH^{+}/B)$ is probably positive in the case of 4-PYMPO-$NH_2$, although lower than that for 4-PYMPO (this point is discussed in the Supporting Information). Thus, the most-stable excited state of 4-PYMPO-$NH_2$ in the pH range between both of the latter $pK_a$ values should be the acidic excited state 4-PYMPOH-$NH_2^{+}$*. Consequently, 4-PYMPO-$NH_2$ singularity is most probably not associated with an absence of $pK_a$ shift upon light absorption.

Finally, one has to examine if 4-PYMPO-$NH_2$ singularity could result from a protonation being too slow during the lifetime of its basic excited state. In fact, the main reactive channels for 4-PYMPO-$NH_2$* protonation should be: 3*1* (reaction with $H^+$), 3*2* (reaction with $H_2O$), and 3*3′* (reaction with the acidic state $YH^+$ of the buffer; Figure 7). Considering that the lifetime of 4-PYMPO-$NH_2$* is in the nanosecond range, when protonation is too slow it means that $\kappa_{(B^*\rightarrow BH^*)}=k_{31}^*H+k_{32}^*+k_{33'}^*YH<\frac{1}{\tau_{(4\text{-PYMPO}^*)}}\approx 10^9\ s^{-1}$. In the case of 4-PYMPO, we showed that protonation in the excited state was dominated by reaction with water in the relevant pH range ($k_{3*2*}=1.8\pm0.7\times10^9\ s^{-1}$). More generally, $k_{3*2*}=k_{2*3*}K_e10^{pK_a(BH^{+}*/B*)}$. Provided that $pK_a(BH^{+}*/B*)<pK_a(H_2O,OH^-)$, $k_{2*3*}$ should be limited by diffusion[25] so $k_{2*3*}\approx10^{10}\ M^{-1}s^{-1}$ in water at room temperature and then $k_{3*2*}\approx10^{pK_a(BH^{+}*/B*)-4}$. From the lifetimes of the basic excited states that share a common nanosecond range, the present oxazoles can be divided into two categories according to the value of $pK_a(BH^{+}*/B*)$. When $pK_a(BH^{+}*/B*)\geq13$, protonation by water can take place during the lifetime of their basic excited state; the opposite is true when $pK_a(BH^{+}*/B*)\leq13$.

Molecules such as 4-PYMPO or 4-PYMPOM clearly exhibit $pK_a(BH^{+}*/B*)\geq13$. As the value of $k_{3*2*}$ can depend on the local structure of water, these molecules should be used with care when measuring the pH by using a ratiometric approach relying on fluorescence emission. In contrast, they could be used as pOH-jump molecules. In the case of 4-PYMPO-$NH_2$, $k_{3*2*}\approx10^{pK_a(BH^{+}*/B*)-4}\approx10^7\ s^{-1}$. Even if $pK_a(BH^+/B)$ is underestimated by 1.4 pH units (see above), one anticipates that $k_{3*2*}\ll\frac{1}{\tau_{(4\text{-PYMPO}^*)}}$. Thus, water has not enough time to protonate 4-PYMPO-$NH_2$* during its lifetime and this absence of protonation is probably responsible of the 4-PYMPO-$NH_2$ singularity. In fact, a rather small difference in $pK_a(BH^{+}*/B*)$ is ultimately revealed as being crucial to determine whether B can be used to perform ratiometric pH measurements relying on fluorescence emission.

Beyond the significance of $k_{32}^*$, it is worth highlighting the other terms contained in $\kappa_{(B^*\rightarrow BH^*)}$ that may also contribute to the protonation of the basic excited state for all of the considered oxazoles, as illustrated in Figure 5b. An upper limit for $k_{31}^*$ and $k_{33'}^*$ is the diffusion limit (typically $10^{10}\ M^{-1}s^{-1}$ in water at room temperature). In relation to biological applications dealing with media that have pH > 4, protonation does not occur at the nanosecond timescale: $k_{31}^*H\ll\frac{1}{\tau_{B^*}}$. In contrast, it is important to underline that $k_{33'}^*YH$ may overcome $\frac{1}{\tau_{B^*}}$ at concentrations in protonated buffer typically exceeding 100 mM.

## Conclusion

This paper accounts for the stepwise design of a reliable fluorescent pH indicator based on a donor–acceptor fluorophore that works close to neutral pH. We showed that the synthetically versatile 5-aryl-2-pyridyloxazoles form an attractive photophysical backbone with tunable acid–base properties. They can be used for optical pH measurements relying on one- and two-photon absorption or on a ratiometric approach based on excitation spectra.

In contrast, the prediction of their emission spectra at a given pH is generally difficult owing to the major change in $pK_a$ experienced upon light absorption. In particular, very different spectra can be obtained in the range between $pK_a$ and $pK_a^*$ depending on the local structure of water, or on the concentration and the $pK_a(YH^+/Y)$ of buffering species. This feature considerably hinders the use of these molecules in ratiometric pH measurements relying on fluorescence emission, in particular, in uncontrolled media such as those encountered in biology. Nevertheless, we identified a 5-aryl-2-pyridyloxazole platform than can also be used to perform ratiometric pH measurements in the pH 3–8 range based on fluorescence emission as a result of a weaker shift of the $pK_a$ upon light absorption. This is especially attractive when two-photon excitation is used because it would allow local addressing on the femtoliter scale. Its similarity to the 4-PYMPO backbone, which was used to design an efficient probe,[10] suggests that 4-PYMPO-$NH_2$ derivatives could be used in applications for measuring intracellular pH.

## Experimental Section

**General procedures**: The commercially available chemicals were used without further purification. Anhydrous solvents were freshly distilled before use. Column chromatography: silica gel 60 (0.040–0.063 mm), Merck. Analytical and thin layer chromatography: silica gel plates, Merck; detection by UV light ($\lambda=254$ nm). Melting point: Büchi 510. $^1H$ NMR spectra: AM-250 or 400 AVANCE Bruker; chemical shifts ($\delta$) in ppm related to protonated solvent as internal reference ($^1H$: $CHCl_3$ in $CDCl_3$, 7.26 ppm; $CHD_2SOCD_3$ in $CD_3SOCD_3$, 2.49 ppm ; HOD in $D_2O$, 4.98 ppm. $^{13}C$: $^{13}CDCl_3$ in $CDCl_3$, 77.0 ppm; $^{13}CD_3SOCD_3$ in $CD_3SOCD_3$, 39.6 ppm); coupling constants $J$ in Hz. Infrared absorption spectra were recorded on a Bruker Tensor 27 spectrometer. Mass spectrometry (chemical ionization with $NH_3$) was performed at the Service de Spectrométrie de masse de l'ENS. Microanalyses were obtained from the Service de Microanalyses de l'Université Pierre et Marie Curie, Paris.

**Syntheses of the precursors for 4-PYMPOM**

*1-Methoxy-2,6-dimethylpyridinium methyl sulfate (**2**)*:[33] Dimethyl sulfate (21.7 mL, 228 mmol, 1 equiv) was poured into 2,6-lutidine-1-oxyde (**1**) (27.6 mL, 228 mmol) slowly enough to prevent the temperature from rising above 80 °C. Then the mixture was stirred at 80 °C for 2 h. After

  

cooling, the precipitate was recrystallized in anhydrous acetone yielding **2** as colorless needles (48.83 g, 86%). $^1$H NMR (250 MHz, $CDCl_3$, 25°C, TMS): $\delta = 8.08$ (t, $^3J = 7.9$ Hz, 1H), 7.67 (d, $^3J = 7.9$ Hz, 2H), 4.23 (s, 3H), 3.39 (s, 3H), 2.74 ppm (s, 6H).

*4-Cyano-2,6-dimethylpyridine (**3**)*:[33] A solution of potassium cyanide (38.26 g, 588 mmol, 3 equiv) in water (80 mL) was added into a solution of **2** (48.83 g, 196 mmol) in water (50 mL) under nitrogen. The resulting mixture was stirred for 24 h at room temperature. After this period, the precipitated pinky powder was collected by filtration and was extracted with dichloromethane for 5 h in a Soxhlet extractor. Compound **3** was eventually obtained as a colorless powder (6.589 g, 25%). The filtrate was extracted three times with diethyl ether (3×50 mL). The organic phases were dried and evaporated yielding a mixture of **3** (4.678 g, 18%) and 2,6-dimethylpyridine (1.708 g) that was not subsequently processed. $^1$H NMR (250 MHz, $CDCl_3$, 25°C, TMS): $\delta = 7.20$ (s, 2H), 2.59 ppm (s, 6H); $^1$H NMR (250 MHz, $D_2O$, 25°C, TMS): $\delta = 7.28$ (s, 2H), 2.39 ppm (s, 6H); $^{13}$C NMR (62.9 MHz, $CDCl_3$, 25°C, TMS): $\delta = 159.4$, 121.7, 120.7, 116.9, 24.5 ppm; IR (ATR): $\tilde{\nu} = 2236$, 1592, 1565, 1399, 1387, 909, 865 cm$^{-1}$; MS (CI, $NH_3$): *m/z* (%): 133 (100) $[M+H]^+$, 124 (21).

*2,6-Dimethylisonicotinic acid (**4**)*: A solution of **3** (3.544 g, 26.8 mmol) and sodium hydroxide (2.145 g, 53.6 mmol, 2 equiv) in ethanol (27 mL) was reacted at reflux for 3 h. After evaporation, the crude residue was dissolved in a minimum of water and 2 M hydrochloric acid was added until pH ≈ 3. The solution was evaporated to dryness. The residue was suspended in hot ethanol (10 mL) and the suspension was filtered. During cooling, **4** recrystallized as colorless crystals (1.553 g, 38%). A second recrystallization was performed on the residue resulting from the evaporation of the ethanol filtrate giving another crop of **4** (1.620 g, 40%). M.p. 283°C (decomp); $^1$H NMR (250 MHz, $D_2O$, 25°C, TMS): $\delta =$ 7.70 (s, 2H), 2.62 ppm (s, 6H); $^{13}$C NMR (62.9 MHz, $D_2O$, 25°C, TMS): $\delta = 170.2$, 153.8, 153.1, 123.3, 18.8 ppm; IR (ATR): $\tilde{\nu} = 3500$–2800, 1630, 1606, 1561, 1410, 790, 758 cm$^{-1}$; MS (CI, $NH_3$): *m/z* (%): 169 (12) $[M+NH]^+$, 152 (100) $[M+H]^+$, 151 (45); elemental analysis calcd (%) for $C_8H_9NO_2$ (151.16) : C 63.56, H 6.00, N 9.26; found: C 63.13, H 6.10, N 9.27.

**Condensations leading to the formation of the 5-aryl-2-aryloxazole ring**

*5-Phenyl-2-(4-pyridyl)oxazole (4-PYPO)*:[24] Isonicotinic acid (1.065 g, 8.6 mmol) was reacted at reflux for 2 h with thionyl chloride (3.1 mL, 43.2 mmol, 5 equiv). After evaporation of the excess thionyl chloride under vacuum, isonicotinoyl chloride chlorhydrate was obtained as a white powder (1.131 g, 73%) that was used in the next step without any further purification.

2-Amino-1-phenylethanone chlorhydrate (1.090 g, 6.3 mmol) was added portionwise to a solution of isonicotinoyl chloride chlorhydrate (1.131 g, 6.3 mmol, 1 equiv) in dry pyridine (18 mL). After warming at 100°C for 2 h, the mixture was cooled to room temperature and poured into water (10 mL). The white precipitate was discarded by means of filtration. After neutralization of the filtrate with solid sodium hydrogencarbonate and filtration, *N*-(phenacyl)isonicotinamide was obtained as orange needles (0.717 g, 47%) that were used without further purification for the next step. $^1$H NMR (400 MHz, $CDCl_3$, 25°C, TMS): $\delta = 8.78$ (AA′XX′, $^3J = 6.0$ Hz, 2H), 8.05–8.01 (m, 2H), 7.71 (AA′XX′, $^3J = 6.0$ Hz, 2H), 7.66 (tt, $^3J = 7.5$ Hz, $^4J = 1.3$ Hz, 1H), 7.57–7.51 (m, 2H), 7.43 (s, 1H), 4.96 ppm (d, $^3J = 4.3$ Hz, 2H); $^{13}$C NMR (100.6 MHz, $CDCl_3$, 25°C, TMS): $\delta = 193.7$, 165.4, 150.7, 140.9, 134.5, 134.0, 129.0, 128.0, 120.9, 46.8 ppm.

A mixture of *N*-(phenacyl)isonicotinamide (717 mg, 3.0 mmol, 1 equiv), acetic anhydride (9 mL), and 85% phosphoric acid (1 mL) was left at reflux for 90 min. After cooling to room temperature, the supernatant was removed. The oily residue was mixed with 6 M sodium hydroxide until pH 8 and a light brownish precipitate was formed after addition of water (5 mL). After filtration and drying, the resulting brown powder was recrystallized in cyclohexane to yield yellow crystals of 4-PYPO (225 mg, 33%). $^1$H NMR (400 MHz, $CDCl_3$, 25°C, TMS): $\delta = 8.76$ (AA′XX′, $^3J = 6.1$ Hz, 2H), 7.94 (AA′XX′, $^3J = 6.2$ Hz, 2H), 7.76–7.72 (m, 2H), 7.52 (s, 1H), 7.50–7.44 (m, 2H), 7.39 ppm (tt, $^3J = 7.4$ Hz, $^4J =$ 1.5 Hz, 1H); $^{13}$C NMR (100.6 MHz, $CDCl_3$, 25°C, TMS): $\delta = 158.7$, 152.6, 150.5, 134.2, 129.1, 129.0, 127.3, 124.5, 124.0, 119.8 ppm; MS (CI, $NH_3$): *m/z* (%): 224 (22), 223 (100) $[M+H]^+$; elemental analysis calcd (%) for $C_{14}H_{10}N_2O$ (222.24): C 75.66, H 4.53, N 12.60; found: C 75.66, H 4.63, N 12.67.

**5-(4′-Methoxyphenyl)-2-aryloxazole rings**: The appropriate acid, 2-amino-1-(4′-methoxyphenyl)ethanone chlorhydrate (1 equiv), and phosphoryl oxychloride $POCl_3$ (8 equiv) were reacted under reflux for 6 h. A precipitate generally started to form at this step. After cooling to room temperature, the excess $POCl_3$ was removed under vacuum. The solution resulting from the addition of ethanol/water (2:1, v/v; just enough to solubilize the residue) to the residue was made basic (pH 8) by adding 28% ammonia. A precipitate formed and was then filtered, washed with water, and dried. It was then recrystallized in cyclohexane.

*5-(4′-Methoxyphenyl)-2-(4-pyridyl)oxazole (4-PYMPO)*:[18] 4-PYMPO was obtained as a fine brown powder (87%). $^1$H NMR (400 MHz, $CDCl_3$, 25°C, TMS): $\delta = 8.74$ (AA′XX′, $^3J = 6.1$ Hz, 2H), 7.91 (AA′XX′, $^3J = 6.2$ Hz, 2H), 7.66 (AA′XX′, $^3J = 8.9$ Hz, 2H), 7.39 (s, 1H), 6.98 (AA′XX′, $^3J = 8.8$ Hz, 2H), 3.86 ppm (s, 3H); $^{13}$C NMR (100.6 MHz, $CDCl_3$, 25°C, TMS): $\delta = 160.3$, 158.1, 152.6, 150.5, 134.3, 126.1, 122.5, 120.1, 119.7, 114.5, 55.4 ppm; elemental analysis calcd (%) for $C_{15}H_{12}N_2O_2$ (252.27): C 71.42, H 4.79, N 11.10; found: C 71.24, H 4.90, N 11.08.

*5-(4′-Methoxyphenyl)-2-(2,6-dimethyl-4-pyridyl)oxazole (4-PYMPOM)*: 4-PYMPOM was obtained as a fine brown powder (60%) that gave a yellow powder after recrystallization in cyclohexane (51%). M.p. 105°C; $^1$H NMR (400 MHz, $CDCl_3$, 25°C, TMS): $\delta = 7.66$ (AA′XX′, $^3J = 8.9$ Hz, 2H), 7.60 (s, 2H), 7.36 (s, 1H), 6.98 (AA′XX′, $^3J = 8.9$ Hz, 2H), 3.86 (s, 3H), 2.60 ppm (s, 6H); $^{13}$C NMR (100.6 MHz, $CDCl_3$, 25°C, TMS): $\delta =$ 160.2, 158.7 (2), 152.3, 134.8, 126.0, 122.3, 120.3, 116.3, 114.5, 55.4, 24.5 ppm; MS (CI, $NH_3$): *m/z* (%): 309 (15), 281 (100) $[M+H]^+$, 280 (13); HRMS (CI, $NH_3$): *m/z* calcd for $C_{17}H_{17}N_2O_2$: 281.1290; found: 281.1286 $[M+H]^+$; elemental analysis calcd (%) for $C_{17}H_{16}N_2O_2$ (280.32): C 72.84, H 5.75, N 9.99; found: C 72.63, H 5.69, N 10.07.

*5-(4′-Methoxyphenyl)-2-(2-chloro-4-pyridyl)oxazole (4-PYMPO-Cl)*: 4-PYMPO-Cl was obtained as a fine yellow powder (88%). $^1$H NMR (250 MHz, $CDCl_3$, 25°C, TMS): $\delta = 8.51$ (d, $^3J = 5.2$ Hz, 1H), 7.96 (s, 1H), 7.85 (d, $^3J = 5.3$ Hz, 1H), 7.68 (AA′XX′, $^3J = 8.8$ Hz, 2H), 7.41 (s, 1H), 7.00 (AA′XX′, $^3J = 8.8$ Hz, 2H), 3.88 ppm (s, 3H); $^{13}$C NMR (62.9 MHz, $CDCl_3$, 25°C, TMS): $\delta = 160.5$, 156.9, 153.2, 152.5, 150.4, 137.1, 126.2, 122.8, 120.3, 119.9, 118.5, 114.6, 55.4 ppm; MS (CI, $NH_3$): *m/z* (%): 289 (35) $[M+H]^+$, 288 (18), 287 (100) $[M+H]^+$, 253 (26); elemental analysis calcd (%) for $C_{15}H_{11}ClN_2O_2$ (286.72): C 62.84, H 3.87, N 9.77; found: C 62.99, H 3.89, N 9.66.

*5-(4′-Methoxyphenyl)-2-(2-pyridyl)oxazole (2-PYMPO)*: 2-PYMPO[51] was obtained as a white powder (63%). $^1$H NMR (400 MHz, $CDCl_3$, 25°C, TMS): $\delta = 8.77$–8.73 (m, $^3J = 4.9$ Hz, 1H), 8.17–8.13 (m, $^3J = 7.0$ Hz, 1H), 7.82 (ddd, $^3J = {}^3J = 7.8$ Hz, $^4J = 1.8$ Hz, 1H), 7.72 (AA′XX′, $^3J =$ 8.8 Hz, 2H), 7.39 (s, 1H), 7.35 (ddd, $^3J = 7.6$, 4.8 Hz, $^4J = 1.1$ Hz, 1H), 6.96 (AA′XX′, $^3J = 8.8$ Hz, 2H), 3.86 ppm (s, 3H); $^{13}$C NMR (100.6 MHz, $CDCl_3$, 25°C, TMS): $\delta = 160.1$, 159.4, 152.6, 150.0, 146.2, 136.8, 126.2, 124.3, 122.3, 121.9, 120.4, 114.3, 55.3 ppm; MS (CI, $NH_3$): *m/z* (%): 254 (29), 253 (100) $[M+H]^+$; elemental analysis calcd (%) for $C_{15}H_{12}N_2O_2$ (252.27) : C 71.42, H 4.79, N 11.10; found: C 71.30, H 4.75, N 11.00.

*5-(4′-Methoxyphenyl)-2-(2-quinolyl)oxazole (2-QUIMPO)*: 2-QUIMPO was obtained as a brown-yellow powder (39%). $^1$H NMR (400 MHz, $CDCl_3$, 25°C, TMS): $\delta = 8.28$–8.25 (m, 3H), 7.87–7.83 (m, 1H), 7.78 (AA′XX′, $^3J = 8.8$ Hz, 2H), 7.78–7.74 (m, 1H), 7.61–7.56 (m, 1H), 7.46 (s, 1H), 6.99 (AA′XX′, $^3J = 8.9$ Hz, 2H), 3.86 ppm (s, 3H); $^{13}$C NMR (100.6 MHz, $CDCl_3$, 25°C, TMS): $\delta = 160.2$, 159.6, 153.1, 148.0, 145.8, 137.0, 130.1, 130.0, 128.1, 127.6, 127.4, 126.4, 122.6, 120.4, 119.3, 114.3, 55.4 ppm; MS (CI, $NH_3$): *m/z* (%): 304 (34), 303 (100) $[M+H]^+$, 141 (17), 110 (18); elemental analysis calcd (%) for $C_{19}H_{14}N_2O_2$ (302.33): C 75.48, H 4.67, N 9.26; found: C 75.46, H 4.84, N 9.10.

*6-[5-(4′-Methoxyphenyl)-2-oxazolyl]picolinic acid (2-PYMPO-$CO_2H$)*: 2,6-Pyridinedicarboxylic acid (1.128 g, 6.75 mmol), 2-amino-1-(4′-methoxyphenyl)ethanone chlorhydrate (1.361 g, 6.75 mmol, 1 equiv), and $POCl_3$ (5.0 mL, 54 mmol, 8 equiv) were reacted under reflux for 3 h. At the end of this step, a solid started to form. After cooling, the mixture

  

was evaporated and an ethanol/water (2:1, v/v; 15 mL) mixture was added to the residue.

The precipitate was filtered, washed with water, and dried; 2,6-bis-[5-(4′-methoxyphenyl)-2-oxazolyl]pyridine was thus obtained as a brown powder (1.034 g, 36%) that was recrystallized in pyridine. $^1$H NMR (400 MHz, $(CD_3)_2SO$, 25°C, TMS): $\delta$ = 8.50–8.46 (m, 2H), 8.41–8.35 (m, 1H), 8.06 (s, 2H), 8.05 (AA′XX′, $^3J$ = 8.8 Hz, 4H), 7.34 (AA′XX′, $^3J$ = 8.8 Hz, 4H), 4.05 ppm (s, 6H); $^{13}$C NMR (100.6 MHz, $(CD_3)_2SO$, 25°C, TMS): $\delta$ = 159.9, 158.4, 152.2, 145.7, 138.8, 126.1, 123.1, 122.8, 119.8, 114.8, 55.4 ppm; elemental analysis calcd (%) for $C_{25}H_{19}N_3O_4$ (425.44): C 70.58, H 4.50, N 9.88; found: C 70.58, H 4.53, N 9.92.

The filtrate was made alkaline (pH 8) by addition of ammonia (28%). The new precipitate was filtered, washed with water, and dried. It was dissolved in a mixture 2M sodium hydroxide (5 mL)/pyridine (1 mL) and the resulting solution was placed at reflux for 1 h to hydrolyze the ester formed during the preceding workup. After cooling, the solution was acidified (to pH 2) with 2M hydrochloric acid yielding a brown powder. 2-PYMPO-$CO_2$H was filtered (500 mg, 25%) and was subsequently recrystallized in an ethanol/water (1.5:1, v/v) mixture. $^1$H NMR (400 MHz, $(CD_3)_2SO$, 25°C, TMS): $\delta$ = 8.55 (dd, $^3J$ = 7.1, 1.8 Hz, 1H), 8.40–8.33 (m, 2H), 8.01 (s, 1H), 8.01 (AA′XX′, $^3J$ = 8.8 Hz, 2H), 7.31 (AA′XX′, $^3J$ = 8.8 Hz, 2H), 4.04 ppm (s, 3H); $^{13}$C NMR (100.6 MHz, $(CD_3)_2SO$, 25°C, TMS): $\delta$ = 165.9, 160.0, 158.5, 152.4, 148.9, 145.5, 139.1, 126.3, 125.7, 125.0, 123.1, 119.9, 114.9, 55.5; MS (CI, $NH_3$): *m*/*z* (%): 315 (27), 314 (100) $[M+NH_4]^+$, 298 (19), 297 (84) $[M+H]^+$, 253 (53); elemental analysis calcd (%) for $C_{16}H_{12}N_2O_4$ (296.28): C 64.86, H 4.08, N 9.45; found: C 64.78, H 4.09, N 9.33.

**Functional alterations of the 5-(4′-methoxyphenyl)-2-aryloxazole derivatives**

*{4-[5-(4′-Methoxyphenyl)-2-oxazolyl]-2-pyridyl}hydrazine (4-PYMPO-NHNH$_2$)*: A mixture of 4-PYMPO-Cl (160 mg, 0.6 mmol, 1 equiv) and hydrazine monohydrate (5 mL, 103.1 mmol) was reacted under reflux for 16 h. After evaporation, the viscous residue was triturated in diethyl ether. The resulting powder was filtered and recrystallized in benzene to yield 4-PYMPO-NHNH$_2$ as a light brown powder (65 mg, 41%). M.p. 160°C; $^1$H NMR (400 MHz, $CDCl_3$, 25°C, TMS): $\delta$ = 8.18 (d, $^3J$ = 5.4 Hz, 1H), 7.66 (AA′XX′, $^3J$ = 8.7 Hz, 2H), 7.46 (s, 1H), 7.32 (dd, $^3J$ = 5.4 Hz, $^4J$ = 1.0 Hz, 1H), 7.24 (d, $^4J$ = 1.2 Hz, 1H), 6.98 (AA′XX′, $^3J$ = 8.7 Hz, 2H), 3.86 ppm (s, 3H); $^{13}$C NMR (62.9 MHz, $(CD_3)_2CO$, 25°C, TMS): $\delta$ = 161.3, 159.8, 153.2, 149.6, 136.7, 127.1, 123.5, 121.3, 115.4, 111.8, 103.4, 55.8 ppm; MS (CI, $NH_3$): *m*/*z* (%): 311 (20), 284 (38), 283 (100) $[M+H]^+$, 282 (23); HRMS (CI, $CH_4$): *m*/*z* calcd for $C_{15}H_{15}N_4O_2$: 283.1195; found: 283.1192 $[M+H]^+$.

*N′-[4-[5-(4′-Methoxyphenyl)-2-oxazolyl]-2-pyridyl}acetohydrazide (4-PYMPO-NHNHAc)*: Acetic anhydride (76.5 mg, 0.75 mmol, 1 equiv) was added to a solution of 4-PYMPO-NHNH$_2$ (211.5 mg, 0.75 mmol, 1 equiv) in pyridine (4 mL). The resulting solution was stirred at room temperature for 33 h. After evaporation, the residue was purified by means of column chromatography on silica gel (dichloromethane/methanol 95:5) to yield 4-PYMPO-NHNHAc as a light yellow powder (200 mg, 82%) that was recrystallized twice: first in benzene and then in chloroform. $^1$H NMR (250 MHz, $CD_3OD$, 25°C, TMS): $\delta$ = 8.23 (d, $^3J$ = 5.4 Hz, 1H), 7.78 (AA′XX′, $^3J$ = 8.8 Hz, 2H), 7.58 (s, 1H), 7.43 (dd, $^3J$ = 5.5 Hz, $^4J$ = 1.2 Hz, 1H), 7.34 (m, 1H), 7.08 (AA′XX′, $^3J$ = 8.8 Hz, 2H), 3.88 ppm (s, 3H); MS (CI, $NH_3$): *m*/*z* (%): 326 (35), 325 (100) $[M+H]^+$, 307 (11), 268 (54), 117 (20); HRMS (CI, $CH_4$): *m*/*z* calcd for $C_{17}H_{17}N_4O_3$: 325.1301; found: 325.1298 $[M+H]^+$.

*4-[5-(4′-Methoxyphenyl)-2-oxazolyl]-2-pyridylamine (4-PYMPO-NH$_2$)*: A suspension of 4-PYMPO-NHNH$_2$ (423 mg, 1.5 mmol) and Raney nickel as a 50% slurry in water (1.5 mL) was stirred under hydrogen ($P$ = 1 bar) at room temperature for 17 h. After filtration over Celite, the filtrate was evaporated. The crude residue was purified by using column chromatography on silica gel (dichloromethane/methanol 95:5) to yield 4-PYMPO-NH$_2$ as a light yellow powder (205 mg, 51%) that was recrystallized in benzene (153 mg, 38%). M.p. 184°C; $^1$H NMR (400 MHz, $CDCl_3$, 25°C, TMS): $\delta$ = 8.19 (d, $^3J$ = 5.4 Hz, 1H), 7.65 (AA′XX′, $^3J$ = 8.8 Hz, 2H), 7.36 (s, 1H), 7.29 (dd, $^3J$ = 5.4, $^4J$ = 1.4 Hz, 1H), 7.16 (m, 1H), 6.98 (AA′XX′, $^3J$ = 8.8 Hz, 2H), 3.87 ppm (s, 3H); $^{13}$C NMR (100.6 MHz, $CDCl_3$, 25°C, TMS): $\delta$ = 160.2, 158.9, 158.6, 152.3, 148.9, 136.1, 126.0, 122.3, 120.3, 114.5, 110.5, 104.6, 55.4; MS (CI, $NH_3$): *m*/*z* (%): 269 (18), 268 (100) $[M+H]^+$; HRMS (CI, $CH_4$): *m*/*z*: calcd for $C_{15}H_{14}N_3O_2$: 268.1086; found: 268.1084 $[M+H]^+$.

*5-(4′-Hydroxyphenyl)-2-(4-pyridyl)oxazole (4-PYHPO)*: A mixture of hydrobromic acid 48% (7 mL), 4-PYMPO (115 mg, 0.45 mmol, 1 equiv), and acetic acid (2 mL) was stirred for 24 h at room temperature. The solution was diluted with water (15 mL) and neutralized with 2M sodium hydroxide until precipitation occurred (pH ≈ 6–7). The fine brown powder was collected (56%, 61 mg) and recrystallized twice in ethanol to yield 4-PYHPO as a cream powder (14%, 15 mg). $^1$H NMR (400 MHz, $CD_3OH$, 25°C, TMS): $\delta$ = 8.89 (AA′XX′, $^3J$ = 6.2 Hz, 2H), 8.23 (AA′XX′, $^3J$ = 6.2 Hz, 2H), 7.88 (AA′XX′, $^3J$ = 8.7 Hz, 2H), 7.74 (s, 1H), 7.10 ppm (AA′XX′, $^3J$ = 8.7 Hz, 2H); $^{13}$C NMR (62.9 MHz, $(CD_3)_2SO$, 25°C, TMS): $\delta$ = 158.3, 157.2, 152.6, 150.6, 133.5, 126.2, 122.5, 119.3, 118.1, 115.9 ppm; MS (CI, $NH_3$): *m*/*z* (%): 240 (26), 239 (100) $[M+H]^+$; HRMS (CI, $NH_3$): *m*/*z* calcd (%) for $C_{14}H_{11}N_2O_2$: 239.0821; found: 239.0820 $[M+H]^+$.

*Methyl ester of 6-[5-(4′-methoxyphenyl)-2-oxazolyl]picolinic acid (2-PYMPO-CO$_2$Me)*: A solution of 2-PYMPO-$CO_2$H (61 mg, 0.2 mmol) and a few drops of concentrated sulfuric acid in methanol (30 mL) was placed under reflux for 1 h. After evaporation of the solvent, the mixture was extracted with water and dichloromethane. The organic phase was dried over anhydrous sodium sulfate to yield 2-PYMPO-$CO_2$Me as a creamy solid after solvent evaporation (55 mg, 86%). M.p. 140°C; $^1$H NMR (250 MHz, $CDCl_3$, 25°C, TMS): $\delta$ = 8.34 (dd, $^3J$ = 8.0 Hz, $^4J$ = 1.0 Hz, 1H), 8.19 (dd, $^3J$ = 8.0 Hz, $^4J$ = 1.0 Hz, 1H), 7.99 (dd, $^3J$ = $^3J$ = 7.8 Hz, 1H), 7.76 (AA′XX′, $^3J$ = 8.8 Hz, 2H), 7.42 (s, 1H), 6.98 (AA′XX′, $^3J$ = 8.8 Hz, 2H), 4.06 (s, 3H), 3.87 ppm (s, 3H); $^{13}$C NMR (62.9 MHz, $CDCl_3$, 25°C, TMS): $\delta$ = 165.4, 160.3, 158.6, 153.2, 148.4, 146.4, 138.0, 126.4, 125.4, 125.0, 122.5, 120.3, 114.4, 55.4, 53.0 ppm; MS (CI, $NH_3$): *m*/*z* (%): 312 (21), 311 (100) $[M+H]^+$.

*6-[5-(4′-Methoxyphenyl)-2-oxazolyl]-2-pyridylmethanol (2-PYMPO-CH$_2$OH)*: Lithium aluminum hydride (1M, 0.46 mL, 0.46 mmol, 1.1 equiv) in THF was added dropwise to a solution of 2-PYMPO-$CO_2$Me (130 mg, 0.42 mmol) in freshly distilled THF (2 mL) under nitrogen. The suspension was stirred at room temperature for 1 h. It was then cautiously neutralized with ammonium chloride. After stirring for 30 min, the organic supernatant was removed and the residue was extracted with diethyl ether. The mixed organic phases were dried over anhydrous sodium sulfate and evaporated. 2-PYMPO-$CH_2$OH was obtained as a yellow powder (95 mg, 80%) that was recrystallized in toluene. $^1$H NMR (250 MHz, $CDCl_3$, 25°C, TMS): $\delta$ = 8.02 (d, $^3J$ = 7.8 Hz, 1H), 7.81 (dd, $^3J$ = $^3J$ = 7.8 Hz, 1H), 7.69 (AA′XX′, $^3J$ = 8.8 Hz, 2H), 7.40 (s, 1H), 7.36 (d, $^3J$ = 7.7 Hz, 1H), 6.97 (AA′XX′, $^3J$ = 8.8 Hz, 2H), 4.88 (s, 2H), 3.86 ppm (s, 3H); $^{13}$C NMR (62.9 MHz, $CDCl_3$, 25°C, TMS): $\delta$ = 160.2, 160.0, 159.2, 152.6, 145.0, 137.6, 132.2, 126.2, 122.3, 121.3, 120.4, 114.5, 64.4, 55.4; MS (CI, $NH_3$): *m*/*z* (%): 284 (18), 283 (100) $[M+H]^+$; elemental analysis calcd (%) for $C_{16}H_{14}N_2O_3$ (282.30): C 68.07, H 5.00, N 9.92; found: C 68.11, H 4.96, N 9.86.

*5-(4′-Methoxyphenyl)-2-[4-(dihydroxyboranyl)]oxazole (4-BOMPO)*: 4-(4,4,5,5-Tetramethyl-1,3,2-dioxaborolan-2-yl)benzoic acid (243 mg, 1.0 mmol) was placed under reflux for 2 h in an excess of thionyl chloride (2 mL, 27 mmol, 28 equiv). After elimination of $SOCl_2$ under vacuum, the crude acyl chloride was dissolved in methylene chloride (50 mL). 2-Amino-1-(4′-methoxyphenyl)ethanone chlorhydrate (195 mg, 1.0 mmol) and pyridine (0.2 mL, 2.95 mmol, 3 equiv) were added to the resulting solution cooled at 0°C and the mixture was stirred for 16 h at room temperature. The organic solution was quenched by addition of water at 0°C and then dried over anhydrous sodium sulfate. After evaporation of the solvent, the crude residue was purified by column chromatography on silica gel (dichloromethane/ethyl acetate 80:20). 2-[4-(4,4,5,5-Tetramethyl-1,3,2-dioxaborolan-2-yl)benzoylamino]-4′-methoxyacetophenone was obtained as a white powder (121 mg, 31%). $^1$H NMR (250 MHz, $CDCl_3$, 25°C, TMS): $\delta$ = 7.92 (AA′XX′, $^3J$ = 8.8 Hz, 2H), 7.85–7.75 (m, AA′XX′, 4H), 7.38–7.28 (m, 1H), 6.91 (AA′XX′, $^3J$ = 8.8 Hz, 2H), 4.83 (d, $^3J$ = 4.1 Hz, 2H), 3.81 (s, 3H), 1.29 ppm (s, 12H); $^{13}$C NMR (62.9 MHz, $CDCl_3$, 25°C, TMS): $\delta$ = 191.6, 166.3, 163.4, 135.1, 134.0, 129.3, 126.3, 125.2, 113.2, 83.1, 54.5, 45.5, 23.9, 23.8 ppm.

  

2-[4-(Dihydroxyboranyl)benzoylamino]-4′-methoxyacetophenone (115 mg, 0.29 mmol, 1 equiv) and phosphorous oxychloride (5 mL, 55 mmol) were refluxed for 90 min. After pouring the mixture onto ice under stirring, a light brown solid started to precipitate. 4-BOMPO was collected by filtration, washed with cold water, and dried by aspiration (65 mg, 76%). $^1$H NMR (250 MHz, $(CD_3)_2SO$, 25°C, TMS): $\delta = 8.05$ (AA′XX′, $^3J = 8.1$ Hz, 2H), 7.96 (AA′XX′, $^3J = 8.1$ Hz, 2H), 7.81 (AA′XX′, $^3J = 8.7$ Hz, 2H), 7.72 (s, 1H), 7.09 (AA′XX′, $^3J = 8.8$ Hz, 2H), 3.84 ppm (s, 3H); $^{13}$C NMR (62.9 MHz, $(CD_3)_2SO$, 25°C, TMS): $\delta =$ 159.7, 159.6, 150.9, 134.7, 128.1, 125.7, 124.6, 122.6, 120.1, 114.6, 55.3 ppm.

*1-Methyl-4-[5-(4′-methoxyphenyl)-2-oxazolyl]pyridinium p-toluenesulfonate (4-PYMPOMe$^+$ TsO$^-$)*:[38] A solution of 4-PYMPO (209 mg, 0.8 mmol) and methyl tosylate (0.2 mL, 1.2 mmol, 1.5 equiv) in toluene (4.2 mL) was placed under reflux for 1 h. The precipitate that was formed after cooling the mixture to room temperature was collected and dried yielding 1-methyl-4-[5-(4′-methoxyphenyl)-2-oxazolyl]pyridinium *p*-toluenesulfonate as a yellow powder (228 mg, 65%). $^1$H NMR (400 MHz, $CDCl_3$, 25°C, TMS): $\delta = 9.18$ (d, $^3J = 6.7$ Hz, 2H), 8.29 (d, $^3J = 6.3$ Hz, 2H), 7.73 (d, $^3J = 8.0$ Hz, 2H), 7.64 (AA′XX′, $^3J = 8.8$ Hz, 2H), 7.50 (s, 1H), 7.08 (d, $^3J = 8.0$ Hz, 2H), 6.96 (AA′XX′, $^3J = 8.8$ Hz, 2H), 4.57 (s, 3H), 3.85 (s, 3H), 2.25 ppm (s, 3H); $^{13}$C NMR (100.6 MHz, $CDCl_3$, 25°C, TMS): $\delta = 161.2$, 156.0, 155.0, 146.6, 143.5, 139.9, 139.4, 128.7, 126.8, 125.8, 124.6, 122.7, 118.7, 114.8, 55.5, 48.5, 21.2 ppm; elemental analysis calcd (%) for $C_{23}H_{22}N_2O_5$ (438.50): C 62.99, H 5.06, N 6.39; found: C 62.58, H 5.34, N 6.19.

**pH measurements**: pH measurements were performed on a standard PHM210 pH meter (Radiometer Analytical) that was calibrated with buffers at pH 4 and 7. For the measurements in the most alkaline solutions (pH > 12), we relied on indicator sticks (precision: ±0.25 pH units).

The evolution of the absorbance or the fluorescence as a function of pH were analyzed with the SPECFIT/32 global analysis system (version 3.0 for 32-bit Windows systems) to extract the p$K_a$ of the ground state.[52] In the case of the excited state, the p$K_a$ was derived either from lifetime measurements (4-PYMPO) or from consideration of the upper pH limit beyond which no further evolution of the fluorescence emission was detected. This was carried out by taking into account that the width over which an observable is affected around the p$K_a$ is 2 pH units (for 2-PYMPO, 2-QUIMPO, and 2-PYMPO-$CH_2OH$) or directly by analyzing the inflection in the titration curve with the SPECFIT/32 software (2-PYMPO-$CO_2$Me).

**Spectroscopic measurements**: Unless stated otherwise, all the experiments were performed at 293 K in Britton–Robinson buffer (boric acid, acetic acid, phosphoric acid), 0.1 M$^{-1}$, prepared according to ref. [53].

**UV/Vis absorption**: UV/Vis absorption spectra were recorded on a Kontron Uvikon-940 spectrophotometer. Molar absorption coefficients were extracted while checking the validity of the Beer–Lambert law.

**Steady-state fluorescence emission**: Corrected fluorescence spectra were obtained from a Photon Technology International LPS 220 spectrofluorimeter. Solutions for fluorescence measurements were adjusted to concentrations such that the absorption was below 0.15 at the excitation wavelength (typical range: a few micromolar). The overall fluorescence quantum yields $\phi_F$ were calculated from the relation given in Equation (4):

$$\phi_F = \phi_{ref} \frac{1-10^{-A_{ref}(\lambda_{exc})}}{1-10^{-A(\lambda_{exc})}} \frac{D}{D_{ref}} \left(\frac{n}{n_{ref}}\right)^2 \quad (4)$$

in which the subscript "ref" stands for standard samples. $A(\lambda_{exc})$ is the absorbance at the excitation wavelength, $D$ is the integrated emission spectrum, and $n$ is the refractive index for the solvent. The uncertainty in the experimental value of $\phi_F$ was estimated to be ±10%. The standard fluorophore for the quantum yield measurements was quinine sulfate in 0.1 M $H_2SO_4$ with $\phi_{ref} = 0.55$.[54]

**Two-photon excitation**: The two-photon excitation spectra were recorded with a homebuilt setup[43] using the reported excitation spectrum of fluorescein for calibration.[22] We investigated the dependence of the fluorescence emission as a function of the excitation power for all the compounds studied and we chose the power such as to remain in the range of power-squared dependence (as a rule, the power before the entrance of the beam expander was set to less than 60 mW).

**Phase-modulation fluorometry**: The time-resolved fluorescence measurements were carried out by using the frequency-domain technique[2] with a phase/modulation instrument Fluorolog3-tau3 (SPEX-JOBIN-YVON). This apparatus works with a xenon lamp as a light source that is modulated by a Pockels cell (accessible range of frequencies: 0.1–300 MHz). POPOP in methanol was used as a reference in the investigated range of emitted wavelengths ($\tau = 1.32$ ns). The excitation wavelength was 360 nm. High-pass filters were used to collect the whole emission from the acidic and basic states of 4-PYMPO ($\lambda > 400$ nm), the selective emission from the acidic state of 4-PYMPO ($\lambda > 550$ nm), and the emission from POPOP ($\lambda > 450$ nm). Absorbances at the excitation wavelength were lower than 0.1 au during this series of experiments.

The fluorescence intensity decays were extracted from the multifrequency data and fitted with a single ($N = 1$) or double ($N = 2$) exponential decay model by using the Globals software (Globals Unlimited, University of Illinois at Urbana Champaign, Laboratory for Fluorescence Dynamics). The fluorescence intensity decay, $I_{pH}(t)$, at a given pH obeys the following [Eq. (5)]:

$$I_{pH}(t) = \sum_{i=1}^{N} a_{i,pH} \exp\left(-\frac{t}{\tau_{i,pH}}\right) \quad (5)$$

in which $a_{i,pH}$ is the pH-dependent amplitude associated with the individual lifetime $\tau_{i,pH}$ ($\sum_{i=1}^{N} a_{i,pH} = 1$). The intensity fraction of the component $i$ in a steady state is given in Equation (6):

$$f_{i,pH} = \frac{\int_0^\infty I_{i,pH}(t)dt}{\int_0^\infty I_{pH}(t)dt} = \frac{a_{i,pH}\tau_{i,pH}}{\sum_{i=1}^{N} a_{i,pH}\tau_{i,pH}} \quad (6)$$

with $\sum_{i=1}^{N} f_{i,pH} = 1$.

## Acknowledgement

Professor W. T. Hynes and Dr. D. Laage are gratefully acknowledged for useful discussions.

[1] J. R. Lakowicz, *Principles of Fluorescence Spectroscopy*, Plenum Press, New York, **1999**.
[2] B. Valeur, *Molecular Fluorescence Principles and Applications*, Wiley-VCH, Weinheim, **2002**.
[3] For a review, see: W. E. Moerner, *J. Phys. Chem. B* **2002**, *106*, 910–927.
[4] W. Denk, J. H. Strickler, W. W. Webb, *Science* **1990**, *248*, 73–76.
[5] C. Xu, W. Zipfel, J. B. Shear, R. M. Williams, W. W. Webb, *Proc. Natl. Acad. Sci. USA* **1996**, *93*, 10763–10768.
[6] R. M. Williams, W. R. Zipfel, W. W. Webb, *Curr. Opin. Chem. Biol.* **2001**, *5*, 603–608.
[7] S. W. Hell, *Nat. Biotechnol.* **2003**, *11*, 1347–1355.
[8] M. Göppert-Mayer, *Ann. Phys.* **1931**, *9*, 273–294.
[9] D. M. Friedrich, *J. Chem. Educ.* **1982**, *59*, 472–481.
[10] Z. Diwu, C.-S. Chen, C. Zhang, D. H. Klaubert, R. P. Haugland, *Chem. Biol.* **1999**, *6*, 411–418.
[11] D. E. Metzler, *Biochemistry The Chemical Reactions of Living Cells, Vol. 1*, 2nd ed., Harcourt-Academic Press, Burlington, Massachusetts, **2001**, p. 295.
[12] J. E. Whitaker, R. P. Haugland, F. G. Prendergast, *Anal. Biochem.* **1991**, *194*, 330–344.

  

[13] S. Charier, O. Ruel, J.-B. Baudin, D. Alcor, J.-F. Allemand, A. Meglio, L. Jullien, *Angew. Chem.* **2004**, *116*, 4889–4892; *Angew. Chem. Int. Ed. Engl.* **2004**, *43*, 4785–4788.
[14] T. Förster, *Z. Elektrochem. Angew. Phys. Chem.* **1950**, *54*, 42–46.
[15] a) A. Weller, *Z. Elektrochem.* **1952**, *56*, 662–668; b) A. Weller, *Z. Phys. Chem. (Muenchen Ger.)* **1955**, *3*, 238–254; c) A. Weller, *Z. Phys. Chem. (Muenchen Ger.)* **1958**, *17*, 224–245.
[16] *Molecular Luminescence Spectroscopy, Methods and Applications*, Part 2 (Ed.: S. G. Schulman), Wiley-Interscience, New York, Chichester, Brisbane, Toronto, Singapore, **1988**, pp. 461–510.
[17] For a recent reference, see: D. Moscovitch, O. Noivirt, A. Mezer, E. Nachliel, T. Mark, M. Gutman, G. Fibich, *Biophys. J.* **2004**, *87*, 47–57.
[18] J. H. Hall, J. Y. Chien, J. M. Kaufman, P. T. Litak, J. K. Adams, R. A. Henry, R. A. Hollins, *J. Heterocycl. Chem.* **1992**, *29*, 1245–1273.
[19] H. J. Lin, P. Herman, J. S. Kang, J. R. Lakowicz, *Anal. Biochem.* **2001**, *294*, 118–125. Note that the molecular formula for DND-160 {2-(4-pyridyl)-5-{[4-(2-dimethylaminoethylaminocarbamoyl)methoxy]-phenyl}oxazole} given in this paper is a 5-(4-pyridyl)-2-(4′-methoxyphenyl)oxazole derivative. In fact, we checked on the Molecular Probes Web site and obtained direct confirmation from this company that the product referenced DND-160 and investigated by these authors was indeed a 2-(4-pyridyl)-5-(4′-methoxyphenyl)oxazole.
[20] R. G. Haugland, *Handbook of Fluorescent Probes and Research Products*, 9th ed., **2002**.
[21] N. DiCesare, J. R. Lakowicz, *Chem. Commun.* **2001**, 2022–2023.
[22] C. Xu, W. W. Webb, *J. Opt. Soc. Am. B* **1996**, *13*, 481–491.
[23] D. D. Perrin, *Dissociation Constants of Organic Bases in Aqueous Solution: Supplement 1972*, Butterworths, London, **1972**.
[24] D. G. Ott, F. N. Hayes, V. N. Kerr, *J. Am. Chem. Soc.* **1956**, *78*, 1941–1944.
[25] M. Eigen, *Angew. Chem.* **1963**, *75*, 489–508.
[26] M. Eigen, W. Kruse, G. Maas, L. de Mayer, *Progress in Reaction Kinetics, Vol. 2* (Ed.: G. Porter), Pergamon Press, Oxford, **1964**, pp. 287–318.
[27] C. Tanford, J. G. Kirkwood, *J. Am. Chem. Soc.* **1957**, *79*, 5333–5339.
[28] C. Tanford, *J. Am. Chem. Soc.* **1957**, *79*, 5340–5347.
[29] L. Jullien, H. Cottet, B. Hamelin, A. Jardy, *J. Phys. Chem. B* **1999**, *103*, 10866–10875.
[30] E. Fluhler, V. G. Burnham, L. M. Loew, *Biochemistry* **1985**, *24*, 5149–5755.
[31] G. Hulbener, A. Lambacher, P. Fromherz, *J. Phys. Chem. B* **2003**, *107*, 7896–7902.
[32] S. Yamaguchi, T. Shirasaka, S. Akiyama, K. Tamao, *J. Am. Chem. Soc.* **2002**, *124*, 8816–8817.
[33] W. E. Feely, E. M. Beavers, *J. Am. Chem. Soc.* **1959**, *81*, 4004–4007.
[34] J. T. Laydon, J. C. Lee, L. M. Hillegass, D. E. Griswold, J. J. Breton, M. C. Chabot-Fletcher, J. L. Adams, *J. Med. Chem.* **1996**, *39*, 3929–3937.
[35] E. E. Glover, M. Yorke, *J. Chem. Soc. C* **1971**, 3280–3285.
[36] K. M. Doxsee, M. Feigel, K. D. Stewart, J. W. Canary, C. B. Knobler, D. J. Cram, *J. Am. Chem. Soc.* **1987**, *109*, 3098–3107.
[37] P. Hamel, D. Riendeau, C. Brideau, C. C. Chan, S. Desmarais, D. Delorme, D. Dube, Y. Ducharme, D. Ethier, E. 43 Grimm, J. P. Falgueyret, J. Guay, T. R. Jones, E. Kwong, M. McAuliffe, C. S. McFarlane, H. Piechuta, M. Roumi, P. Tagari, R. N. Young, Y. Girard, *J. Med. Chem.* **1997**, *40*, 2866–2875.
[38] D. G. Ott, F. N. Hayes, V. N. Kerr, *J. Am. Chem. Soc.* **1960**, *82*, 186–189.
[39] C. A. Reichardt, *Solvents and Solvent Effects in Organic Chemistry*, 3rd ed., VCH, Weinheim, **2003**.
[40] D. Laage, W. H. Thompson, M. Blanchard-Desce, J. T. Hynes, *J. Phys. Chem. A* **2003**, *107*, 6032–6046.
[41] Z. Diwu, Y. Lu, C. Zhang, D. H. Klaubert, R. P. Haugland, *Photochem. Photobiol.* **1997**, *66*, 424–431.
[42] N. DiCesare, J. R. Lakowicz, *J. Phys. Chem. A* **2001**, *105*, 6834–6840.
[43] E. Cogné-Laage, J.-F. Allemand, O. Ruel, J.-B. Baudin, V. Croquette, M. Blanchard-Desce, L. Jullien, *Chem. Eur. J.* **2004**, *10*, 1445–1455.
[44] The cross section for two-photon absorption of the pyranin backbone was deduced from the measurements of the product $\delta_{max}\phi_F$ by Xu and Webb (ref. [22]) after introduction of the quantum yield $\phi_F$ of the investigated cascade blue derivative provided by the Molecular Probes Company under comparable conditions.
[45] M. H. V. Werts, S. Gmouh, O. Mongin, T. Pons, M. Blanchard-Desce, *J. Am. Chem. Soc.* **2004**, *126*, 16294–16295.
[46] S. J. K. Pond, O. Tsutsumi, M. Rumi, O. Kwon, E. Zojer, J.-L. Brédas, S. R. Marder, J. W. Perry, *J. Am. Chem. Soc.* **2004**, *126*, 9291–9306.
[47] H. M. Kim, M.-Y. Jeong, H. C. Ahn, S.-J. Jeon, B. R. Cho, *J. Org. Chem.* **2004**, *69*, 5749–5751.
[48] L. M. Tolbert, K. M. Solntsev, *Acc. Chem. Res.* **2002**, *35*, 19–27.
[49] We used a three-component buffer (boric acid, acetic acid, phosphoric acid) during our experiments.[53] For the convenience of the analysis, we assumed that they shared identical rate constants for reaction with 4-PYMPO* ($k_{33'}$) and 4-PYMPOH$^+$* ($k_{3'3}$). This hypothesis is reasonable for "normal" acid–base couples.[25] Then we calculated the concentration in both the acidic and basic state of our "buffer YH$^+$/Y" at any pH by taking into account the respective p$K_a$ of the three components.
[50] H. Eyring, J. Walter, G. E. Kimball, *Quantum Chemistry*, 10th ed., Wiley, New York, **1961**.
[51] D. G. Ott, F. N. Hayes, E. Hansbury, V. N. Kerr, *J. Am. Chem. Soc.* **1957**, *79*, 5448–5454.
[52] a) H. Gampp, M. Maeder, C. J. Meyer, A. D. Zuberbühler, *Talanta* **1985**, *32*, 95–101; b) H. Gampp, M. Maeder, C. J. Meyer, A. D. Zuberbühler, *Talanta* **1985**, *32*, 257–264; c) H. Gampp, M. Maeder, C. J. Meyer, A. D. Zuberbühler, *Talanta* **1985**, *32*, 1133–1139; d) H. Gampp, M. Maeder, C. J. Meyer, A. D. Zuberbühler, *Talanta* **1986**, *33*, 943–951.
[53] C. Frugoni, *Gazz. Chim. Ital.* **1957**, *87*, 403–407.
[54] J. N. Demas, G. A. Crosby, *J. Phys. Chem.* **1971**, *75*, 991–1024.

Received: June 1, 2005
Published online: October 25, 2005

  